ISSN 2644-3260 (online)

Artificial Intelligence in *Medical Imaging*

Artif Intell Med Imaging 2021 June 28; 2(3): 56-85

Published by Baishideng Publishing Group Inc

AIMI

Artificial Intelligence in Medical Imaging

Contents

Bimonthly Volume 2 Number 3 June 28, 2021

Artificial Intelligence in Medical Imaging

Bimonthly Volume 2 Number 3 June 28, 2021

Contents

ABOUT COVER

Editorial board member of *Artificial Intelligence in Medical Imaging*, Quan Zhou, MD, Professor, Department of Medical Imaging, The Third Affiliated Hospital of Southern Medical University, Guangzhou 510630, Guangdong Province, China

AIMS AND SCOPE

The primary aim of *Artificial Intelligence in Medical Imaging* (*AIMI*, *Artif Intell Med Imaging*) is to provide scholars and readers from various fields of artificial intelligence in medical imaging with a platform to publish high-quality basic and clinical research articles and communicate their research findings online.

AIMI mainly publishes articles reporting research results obtained in the field of artificial intelligence in medical imaging and covering a wide range of topics, including artificial intelligence in radiology, pathology image analysis, endoscopy, molecular imaging, and ultrasonography.

INDEXING/ABSTRACTING

There is currently no indexing.

RESPONSIBLE EDITORS FOR THIS ISSUE

Production Editor: *Yan-Xia Xing*; **Production Department Director:** *Yu-Jie Ma*; **Editorial Office Director:** *Yun-Xiaojiao Wu*.

NAME OF JOURNAL
Artificial Intelligence in Medical Imaging

ISSN
ISSN 2644-3260 (online)

LAUNCH DATE
June 28, 2020

FREQUENCY
Bimonthly

EDITORS-IN-CHIEF
Xue-Li Chen, Caroline Chung, Jun Shen

EDITORIAL BOARD MEMBERS
https://www.wjgnet.com/2644-3260/editorialboard.htm

PUBLICATION DATE
June 28, 2021

INSTRUCTIONS TO AUTHORS
https://www.wjgnet.com/bpg/gerinfo/204

GUIDELINES FOR ETHICS DOCUMENTS
https://www.wjgnet.com/bpg/GerInfo/287

GUIDELINES FOR NON-NATIVE SPEAKERS OF ENGLISH
https://www.wjgnet.com/bpg/gerinfo/240

PUBLICATION ETHICS
https://www.wjgnet.com/bpg/GerInfo/288

PUBLICATION MISCONDUCT
https://www.wjgnet.com/bpg/gerinfo/208

ARTICLE PROCESSING CHARGE
https://www.wjgnet.com/bpg/gerinfo/242

STEPS FOR SUBMITTING MANUSCRIPTS
https://www.wjgnet.com/bpg/GerInfo/239

ONLINE SUBMISSION
https://www.f6publishing.com

Artificial Intelligence in Medical Imaging

Submit a Manuscript: https://www.f6publishing.com

Artif Intell Med Imaging 2021 June 28; 2(3): 56-63

DOI: 10.35711/aimi.v2.i3.56

ISSN 2644-3260 (online)

OPINION REVIEW

Implementation of lung ultrasound in the triage of pregnant women during the SARS-CoV-2 pandemics

Arzu Bilge Tekin, Murat Yassa

ORCID number: Arzu Bilge Tekin 0000-0001-8054-2624; Murat Yassa 0000-0001-8661-1192.

Author contributions: Tekin AB and Yassa M contributed equally to this work; Tekin AB and Yassa M performed the research, analyzed the data and wrote the manuscript; all authors have read and approved the final manuscript.

Conflict-of-interest statement: The authors report no conflict of interest.

Manuscript source: Invited manuscript

Specialty type: Obstetrics and gynecology

Arzu Bilge Tekin, Murat Yassa, Department of Obstetrics and Gynecology, Sancaktepe Sehit Prof. Dr. Ilhan Varank Training and Research Hospital, Istanbul 34785, Sancaktepe, Turkey

Corresponding author: Arzu Bilge Tekin, MD, Associate Specialist, Department of Obstetrics and Gynecology, Sancaktepe Sehit Prof. Dr. Ilhan Varank Training and Research Hospital, Emek Mahallesi, Namık Kemal Caddesi No. 54, Istanbul 34785, Sancaktepe, Turkey. arzubilgetekin@gmail.com

Abstract

Lung ultrasound (US) has been shown that it is able to detect interstitial lung disease, subpleural consolidations and acute respiratory distress syndrome in clinical and physical studies that assess its role in upper respiratory infections. It is used worldwide in the coronavirus disease 2019 (COVID-19) outbreak and the effectiveness has been assessed in several studies. Fast diagnosis of COVID-19 is essential in deciding for patient isolation, clinical care and reducing transmission. Imaging the lung and pleura by ultrasound is efficient, cost-effective, and safe and it is recognized as rapid, repeatable, and reliable. Obstetricians are already using the US and are quite proficient in doing so. During the pandemic, performing lung US (LUS) right after the fetal assessment until reverse transcription polymerase chain reaction results are obtained, particularly in settings that have a centralized testing center, was found feasible for the prediction of the severe acute respiratory syndrome coronavirus 2 (SARS-CoV-2) infection. The use of LUS is efficient in the triage and monitoring of pregnant women. Clinicians dealing with pregnant women should consider LUS as the first-line diagnostic tool in pregnant women during the SARS-CoV-2 pandemic.

Key Words: COVID-19 pandemics; Lung; Ultrasound imaging; Pregnancy; SARS-CoV-2; Triage

Core Tip: Lung ultrasound (US) is based on specific pattern recognition and does not require complex measurements, therefore obstetricians can easily learn and use lung ultrasound (LUS) in the pandemic. LUS examination can be a routine after a routine obstetric US examination. Fast diagnosis of coronavirus disease 2019 is essential in

Country/Territory of origin: Turkey

Peer-review report's scientific quality classification
Grade A (Excellent): 0
Grade B (Very good): B
Grade C (Good): 0
Grade D (Fair): D
Grade E (Poor): 0

Received: April 10, 2021
Peer-review started: April 10, 2021
First decision: April 28, 2021
Revised: May 6, 2021
Accepted: June 4, 2021
Article in press: June 4, 2021
Published online: June 28, 2021

P-Reviewer: Samadder S, Thandassery RB
S-Editor: Fan JR
L-Editor: Filipodia
P-Editor: Xing YX

deciding for patient isolation, clinical care, and reducing transmission. Clinicians dealing with pregnant women should consider LUS as the first-line diagnostic tool in pregnant women during the severe acute respiratory syndrome coronavirus 2 pandemic.

Citation: Tekin AB, Yassa M. Implementation of lung ultrasound in the triage of pregnant women during the SARS-CoV-2 pandemics. *Artif Intell Med Imaging* 2021; 2(3): 56-63
URL: https://www.wjgnet.com/2644-3260/full/v2/i3/56.htm
DOI: https://dx.doi.org/10.35711/aimi.v2.i3.56

INTRODUCTION

Lung ultrasound (US) use has been discussed for years in emergency medicine, intensive care units, and cardiovascular diseases. The use of lung US (LUS) has increased in the last 15-20 years upon advancements in the visualization of pleural effusions, lung masses, and afterward evolved to be able to evaluate lung parenchyma mainly as a point-of-care technique[1]. Pulmonologists, emergency medicine physicians, thoracic and cardiac surgeons often benefit from LUS in the management of traumatic conditions and intraoperative situations[2]. Coronavirus disease 2019 (COVID-19) pneumonia mainly involves the lung periphery and causes interstitial pneumonia. Therefore, LUS is highly suitable for the management of this disease[3]. The obstetricians are already familiar with the US and they are at the frontline in the fight against the severe acute respiratory syndrome coronavirus 2 (SARS-CoV-2) pandemic for infected pregnant women treatment[4]. LUS is based on specific pattern recognition and does not require complex measurements, therefore the obstetricians can easily learn and use LUS in the pandemic[1,5].

SCORING SYSTEM FOR LUS

LUS has been shown that it is able to detect interstitial lung disease, subpleural consolidations and acute respiratory distress syndrome in clinical and physical studies that assess its role in upper respiratory infections[6-8]. It is widely used worldwide in the COVID-19 outbreak and the effectiveness has been assessed in several studies[9-14]. LUS evaluation covers 14 anatomical regions, 3 posterior, 2 lateral, 2 anterior, in both hemithorax and intercostal spaces in supine, right lateral, left lateral positions during at least 10 s[6]. In different scoring systems, the target regions were varied between 4 to 7 regions for each hemithorax[15]. Pleural thickness, pleural continuity, pleural drift (with inspiration and expiration), presence of subpleural consolidated areas, parenchymal artifacts (vertical, horizontal), and the presence of a white lung pattern should be focused in every region. The results of 14 anatomical regions are scored between 0 and 3; LUS 0 is defined as normal LUS findings, LUS score of 1 is defined as mild involvement, LUS score of 2 is defined as moderate involvement and LUS score of 3 is defined as severe lung involvement[6]. Normal US findings (LUS 0) represent thin, continuous, and regular pleural lines, presence of respiratory pleural shift and parenchymal horizontal artifacts due to normally aerated lung surface reflectivity (A lines) in LUS. Mild involvement (LUS 1) is defined with an indented pleural line (irregularities in the pleural line, continuity is not broken), the sporadic vertical white area under the pleura (B line). Moderate involvement (LUS 2) is defined with broken pleura (continuity disorder in the pleural line), small to the large white area of consolidation under pleura, and multiple white vertical lines (B lines) that progress to the end of the viewed area. Severe lung involvement (LUS 3) is defined as a severe broken pleura pattern in addition to a dense and wide "white lung" pattern with or without consolidated area in LUS[6]. B lines, small consolidated areas and broken pleural lines are suggestive of COVID-19[16]. Bacterial pneumonia is mainly represented with isolated large lobar consolidation with or without pleural effusion and dynamic air bronchograms[17].

ADVANTAGES OF LUS

Fast diagnosis of COVID-19 is essential in deciding for patient isolation, clinical care and reducing transmission. For diagnosis of COVID-19, symptoms are leading us and mainly reverse transcription polymerase chain reaction (RT-PCR) testing is the first choice for definitive diagnosis. However, the sensitivity of the SARS-CoV-2 RT-PCR which is the gold standard for diagnosis is estimated as 75%[18]. Furthermore, RT-PCR results may need several days and cannot be sufficient in places with high patient density[18]. Concerning radiologic diagnosis of COVID-19 is based on chest computed tomography (CT) with typical ground-glass opacities and patchy infiltrates in chest radiography, or both[10]. The main advantage of LUS is not only reducing the exposure to ionizing radiation but also reducing the risk of contamination and decrease the burden on the health system. Moreover, it enables monitoring (repetitive measurements)[4,9-11]. However, CT has disadvantages of ionizing radiation exposure, the need for extensive decontamination and is unobtainable in resource-limited situations. Owing to these facts, CT is not an optimal screening tool and not feasible in monitoring the patient's clinical situation[18]. Especially when we think of a special population such as pregnant women or pediatric patients, CT is not an attractive choice for the diagnosis of lung involvement. A low level of ionizing radiation exposure by chest imaging during pregnancy is considered relatively safe, but this can cause anxiety for many pregnant women and health care providers[10]. More than half of the pregnant women refused to have the chest CT in our center (unpublished data).

Imaging the lung and pleura by the US is efficient, cost-effective, and safe, and it is recognized as rapid, repeatable, and reliable[8]. LUS is convenient for bedside evaluation of patients and suitable for vulnerable populations such as pregnant women and children[11,19]. It is already well-known that LUS has the advantages of being a non-ionizer, rapid and easy to perform, and provides dynamic imaging. In addition, LUS has a value and an advantage of applicability to a variety of practice environments, when the other diagnostic tools are unavailable[18].

Obstetricians are already using the US and quite proficient in the use of it. During the pandemic, it was proposed that LUS may be performed by obstetricians and therefore, LUS examination can be a routine after a routine obstetric US examination [4]. This approach might have an impact on reducing the workload of radiologists and the need for chest CT, thereby minimizing the risk of transmission. Pregnant and non-pregnant women have previously been reported to be similar with regard to radiologic findings of COVID-19[10,20]. Performing LUS right after the fetal assessment until RT-PCR results are obtained, particularly in settings that have a centralized testing center, was found feasible for the prediction of the SARS-CoV-2 infection. This approach is successful in reducing the use of chest CT or X-rays for pregnant women.

TRIAGE WITH LUS

Despite the extensive use of LUS in clinical studies, the use of LUS in the triage of pregnant women during the COVID-19 pandemic is still scarce in the literature.

One of the main problems in the management of the population during the SARS-CoV-2 pandemic is to determine the asymptomatic carriers[21]. This issue becomes prominent in pregnant women due to the mixed symptoms that can naturally be interpreted as common complaints of pregnancy. In a recent study by Sutton *et al*[21], the asymptomatic carrier rate in the labor ward was found as 13.7%. Another milestone study from Vintzileos *et al*[22] showed that two-thirds of all pregnant women infected with SARS-CoV-2 were asymptomatic during admission to the labor ward unit. Those results have raised concerns about the high rate of asymptomatic carriers during intensely progressing pandemic.

In our clinic, patients with symptoms are isolated in the hospital until SARS-CoV-2 RT-PCR results are obtained. Asymptomatic pregnant women are initially triaged using LUS and their clinic management is adjusted according to the obtained LUS score. Asymptomatic patients with mild lung involvement were closely followed up until RT-PCR results with home isolation and further close monitoring with LUS is planned. Pregnant women with moderate or severe lung involvement in US receive medical treatment regardless of being symptomatic or asymptomatic. Possible false-negative cases, that are symptomatic with initial normal LUS findings are scheduled for a repeat US in 3 d and offered for Chest CT. This algorithm is schematized in Figure 1.

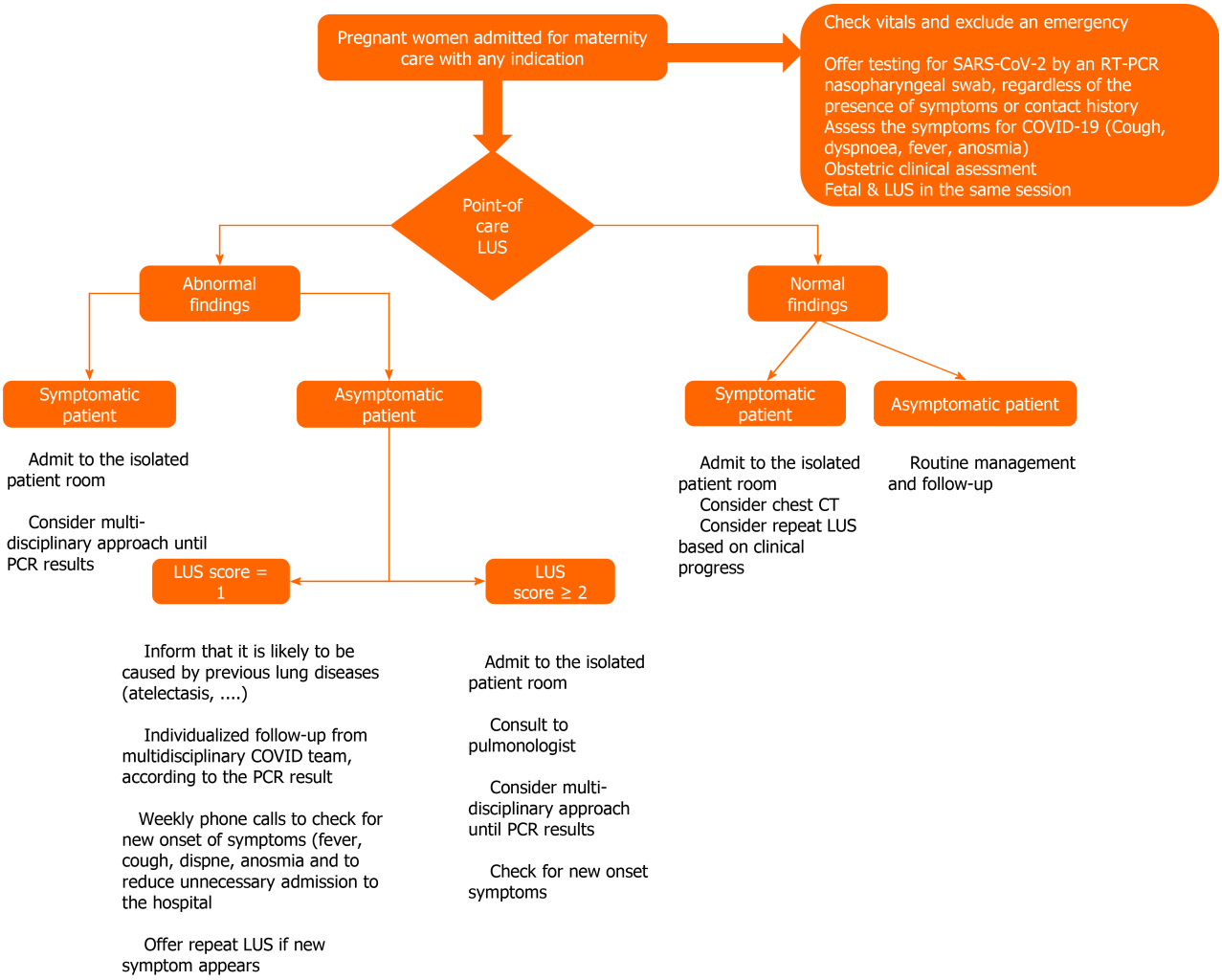

Figure 1 Main triage algorithm of pregnant women based on lung ultrasound. COVID: Coronavirus disease; COVID-19: Coronavirus disease 2019; CT: Computed tomography; LUS: Lung ultrasound; PCR: Polymerase chain reaction; SARS-CoV-2: Severe acute respiratory syndrome coronavirus 2.

Pregnant women are vulnerable population that possess medical and social burdens. In the COVID-19 pandemic, they require several encounters with the healthcare staff, and most of them are hospitalized for birth[23]. The common physiological changes of pregnancy may coincide with the symptoms of COVID-19 infection and undetected cases of COVID-19 were 4-9 cases to 1 detected case in a study in the labor ward[24]. The undetected infection has been thought to contribute to the transmission of the virus[25]. Due to the excess of undetected cases and transmission of infection from asymptomatic carriers, the need for universal screening of pregnant women is emphasized[21,22]. All pregnant women should be offered RT-PCR testing for SARS-CoV-2 infection regardless of the maternal symptoms on admission to the hospital according to the Royal College of Obstetricians & Gynecologists statement[26]. Our study investigating the universal testing strategy for SARS-CoV-2 infection with RT-PCR in pregnant women who were admitted to the hospital showed an overall and asymptomatic infection diagnosis rate of 7.77% and 4.05%, respectively[27]. The false positivity of LUS was due to previous benign lung diseases where the main maternal symptom status comes forward in the interpretation of LUS findings[27]. In our routine approach, LUS comes prior to the maternal symptomatology because mild COVID-19 symptoms can interfere with the natural pregnancy-related symptoms, moreover, we observed that LUS signs can alert the clinician before bothersome symptoms occur. In our algorithm for the interpretation of LUS findings that combines the lung imaging and the maternal symptomatology; a LUS score of 1 was accepted as a normal finding in asymptomatic pregnant women with aiming to reduce the false positivity of LUS imaging. LUS scores of 2 and 3 were adopted as abnormal regardless of the symptom status. In addition, using LUS in the triage of pregnant women was found more predictive in detecting the infection than the use of symptomatology solely with a positive predictive value and sensitivity of

82.3% and 60.9%, respectively[27].

MONITORING WITH LUS AND OTHER AREAS OF USE

In monitoring the clinical progress of pregnant women, LUS is a harmless choice and valuable in terms of deciding either delivery or upgrade the medical treatment[10]. LUS is a very practical alternative in the respiratory system propaedeutic as it allows for repetition of exams, can be portable and performed at the patient's bedside[15]. The recent study suggested the integration of LUS into the routine clinical management of COVID-19[28]. In addition, this recent study emphasized in the emergency department that LUS may correctly triage patients according to their degree of lung involvement[28]. Abnormal LUS findings were reported as relevant with early admission into emergency units or intensive care units[27]. It is reasonable to offer LUS for the triage and monitoring of the clinical progress of patients with leaving the indication of chest CT scan as reserved only for the more complex cases, such as unexpected deterioration in clinical progress and patients with previous lung diseases[28]. Moreover, the detection power for the presence of consolidations there was found in a good agreement between the chest CT and LUS[29]. The studies regarding LUS usage in pregnant women are summarized in Table 1[10,27,30-36].

Considering the patients who are receiving respiratory support is recommended that they should be monitored closely for clinical deterioration[37]. In this regard, serial LUS is suitable for efficient monitoring[37]. The decision to proceed with invasive mechanical ventilation and intubation can be a challenging choice and LUS might be an accurate indicator of the ideal moment of intubation[37]. In intubated patients, LUS could evaluate the pulmonary aeration loss and ventilation condition dynamically thus, enabling the prediction of the healing process[37]. In intensive care units, chest CT scan is risky for transporting critically unwell patients, and decontamination is a time-consuming process[37]. The use of portable chest radiographs is not suitable due to the poor correlation with clinical picture[37].

LIMITATIONS OF LUS

Despite the several advantages of LUS in the COVID-19 pandemic setting, the diagnostic accuracy of LUS may be affected by the patient's characteristics and comorbidities including elevated body-mass index and pre-existing interstitial lung diseases[38,39]. The findings of preexisting interstitial inflammation, scarring, and pleural thickening can mimic the initial COVID-19 imaging. In addition, heart failure causing pulmonary edema or end-stage renal disease may lead to diagnostic confusion with the interstitial inflammation caused by COVID-19. Approximately 70% of the lung surface can be visualized with a systematic LUS examination, however, lesions located in the blind area of the US can be missed[31].

The studies investigating the use of LUS in the COVID-19 pandemic have included small sample sizes and much effort is needed to increase the quality of those studies to promote the LUS scanning in the triage of COVID-19[15]. The specific protocols for triage should be formed and the effects of the clinicians' experience and the inter-operator agreement should be further studied[40-42].

User-related limitations can be challenging in the management of the patient that depends on the LUS scores. It is postulated that less-experienced users are tended to label the mild abnormalities in a single lung field as compatible with COVID-19. The US settings of the LUS can affect the interpretation of LUS images such as undergained or overgained images may lead to false-negative or positive assessments[18].

CONCLUSION

LUS is promising in the management of pregnant women with COVID-19 with considering the advantages of being non-ionizer, dynamic, rapid, reliable, and reproducible. The use of LUS seems efficient in the triage and monitoring of pregnant women. LUS scanning can be combined with initial maternal symptom status in order to reduce the false positivity of LUS. Clinicians dealing with pregnant women may consider LUS as the first-line diagnostic tool in pregnant women during the SARS-CoV-2 pandemic.

Table 1 Studies reported the use of lung ultrasound in pregnant women with coronavirus disease 2019

Ref.	Country	Type of study	Cohort	Diagnosis	LUS technic	Conclusion
Buonsenso *et al*[30], 2020	Italy	Case report	4 pregnant women at 24, 38, 17, and 35 wk gestational age	LUS was carried out before the positive RT-PCR result. Nasopharyngeal swab RT-PCR confirmation	14 regions evaluation with the convex probe.	LUS was correlated with CT findings, this tool should be considered in clinical deterioration to check the lung status for COVID-19 pneumonia and LUS might be preferred to chest X-ray in pregnant women
Deng *et al* [31], 2021	China	Retrospective study	27 of pregnant women at the third trimester, 8 of them at the second trimester, and 4 of them at the first trimester	29 of them with pharynx RT-PCR testing and 10 with epidemiologic history, symptoms, and imaging results	12 zones: 2 anterior zones, 2 lateral zones, and 2 posterior zones *per* side. Each zone was scored 0 to 3 and total LUS scores were used in the clinical assessment of patients	Quantitative LUS can be considered a reliable follow-up tool for dynamic lung monitoring in pregnant women with COVID-19 and can reduce the use of chest CT
Gil-Rodrigo *et al*[32], 2021	Spain	Letter to the editor	4 women at gestational weeks 6, 9, 19 and 25, 2 of them confirmed as COVID-19	Symptoms and LUS were used as initial assessment and nasopharyngeal swab RTPCR was used for confirmation	With convex transducer, 8 posterior lung areas	With regard to potential disease transmission during a pandemic, LUS in pregnant women enables safe diagnosis and early treatment. One of the limitations is the absence of standardized training, the learning curve is relatively
Inchingolo *et al*[33], 2020	Italy	Case report	1 pregnant woman at 23 wk gestational age	Oropharyngeal swab RT-PCR	14 regions with Convex wireless transducer (3.5 MHz)	Point-of-care LUS examination could play a key role in the assessment of pregnant women with suspected COVID-19
Kalafat E *et al* [34], 2020	Turkey	Case report	32-yr-old woman at 35 + 3 wk gestational age	Symptoms and lung ultrasound findings first and confirmed by nasopharyngeal RT-PCR after	Thick and bilateral B-lines in the basal posterior lungs area (during the first assessment), diffuse B-lines (2 d later)	Report of positive lung ultrasound findings consistent with COVID-19 in a pregnant woman with an initially negative RT-PCR result
Porpora *et al* [35], 2021	Italy	Prospective observational study	30 pregnant women at 36 wk of median gestational age (range between 28-38 wk)	Nasopharyngeal swab RT-PCR	Linear or convex probes, the LUS investigation was carried out with the 12-zone method, both in the supine and lateral positions	LUS is proven to be safe, reliable, sensitive, easily repeatable, and could be a guide to define the most appropriate strategy for improving clinical and pregnancy outcomes
Yassa *et al* [10], 2021	Turkey	Case series	8 Pregnant women (9-38 wk) who underwent LUS examinations after obstetric US examinations	Symptoms and LUS first and confirmed by nasopharyngeal RT-PCR testing later	Fourteen areas (3 posterior, 2 lateral, and 2 anterior) were scanned *per* patient for 10 seconds along the indicated lines	After an obstetric US assessment, the routine use of LUS can substantially influence the clinical treatment of pregnant women with COVID-19
Yassa *et al* [27], 2020	Turkey	Prospective Cohort	296 pregnant women (23 with a positive result for COVID-19) at 5 to 42 wk gestational ages (mean = 35.18 wk)	LUS first and confirmed by nasopharyngeal RT-PCR later	12 areas, with the posterior ones in the posterior axillary line	Using lung ultrasound was found more predictive in detecting the infection than the use of symptomatology solely
Youssef *et al* [36], 2020	Italy	Case report	1 pregnant woman, 33 yr old at 26 wk of gestational age	LUS findings were former, positive nasopharyngeal swab RTPCR confirmation later	6 regions in each hemithorax (2 anterior, 2 lateral, and 2 posterior). Linear or convex probes	We believe that extensive training of physicians may be considerably helpful in terms of the ongoing pandemic of COVID-19

COVID-19: Coronavirus disease 2019; CT: Computed tomography; LUS: Lung ultrasound; RT-PCR: Reverse transcription polymerase chain reaction; US: Ultrasound.

REFERENCES

1 **Gargani L**, Volpicelli G. How I do it: lung ultrasound. *Cardiovasc Ultrasound* 2014; **12**: 25 [PMID: 24993976 DOI: 10.1186/1476-7120-12-25]

2 **Francisco Neto MJ**, Rahal Junior A, Vieira FAC, Silva PSDd, Funari MBdG. Advances in lung ultrasound. *Einstein (Sao Paulo)* 2016; **14**: 443-448 [DOI: 10.1590/S1679-45082016MD3557]

3 **Kuzan TY**, Murzoğlu Altıntoprak K, Çiftçi HÖ, Kuzan BN, Yassa M, Tuğ N, Çimşit NÇ. Clinical and radiologic characteristics of symptomatic pregnant women with COVID-19 pneumonia. *J Turk Ger Gynecol Assoc* 2021 [PMID: 33631874 DOI: 10.4274/jtgga.galenos.2021.2020.0215]

4 **Moro F**, Buonsenso D, Moruzzi MC, Inchingolo R, Smargiassi A, Demi L, Larici AR, Scambia G, Lanzone A, Testa AC. How to perform lung ultrasound in pregnant women with suspected COVID-19. *Ultrasound Obstet Gynecol* 2020; **55**: 593-598 [PMID: 32207208 DOI: 10.1002/uog.22028]

5 **Yassa M**, Mutlu MA, Kalafat E, Birol P, Yirmibeş C, Tekin AB, Sandal K, Ayanoğlu E, Yassa M, Kılınç C, Tug N. How to perform and interpret the lung ultrasound by the obstetricians in pregnant women during the SARS-CoV-2 pandemic. *Turk J Obstet Gynecol* 2020; **17**: 225-232 [PMID: 33072428 DOI: 10.4274/tjod.galenos.2020.93902]

6 **Soldati G**, Smargiassi A, Inchingolo R, Buonsenso D, Perrone T, Briganti DF, Perlini S, Torri E, Mariani A, Mossolani EE, Tursi F, Mento F, Demi L. Proposal for International Standardization of the Use of Lung Ultrasound for Patients With COVID-19: A Simple, Quantitative, Reproducible Method. *J Ultrasound Med* 2020; **39**: 1413-1419 [PMID: 32227492 DOI: 10.1002/jum.15285]

7 **Soldati G**, Demi M, Smargiassi A, Inchingolo R, Demi L. The role of ultrasound lung artifacts in the diagnosis of respiratory diseases. *Expert Rev Respir Med* 2019; **13**: 163-172 [PMID: 30616416 DOI: 10.1080/17476348.2019.1565997]

8 **Mayo PH**, Copetti R, Feller-Kopman D, Mathis G, Maury E, Mongodi S, Mojoli F, Volpicelli G, Zanobetti M. Thoracic ultrasonography: a narrative review. *Intensive Care Med* 2019; **45**: 1200-1211 [PMID: 31418060 DOI: 10.1007/s00134-019-05725-8]

9 **Soldati G**, Smargiassi A, Inchingolo R, Buonsenso D, Perrone T, Briganti DF, Perlini S, Torri E, Mariani A, Mossolani EE, Tursi F, Mento F, Demi L. Is There a Role for Lung Ultrasound During the COVID-19 Pandemic? *J Ultrasound Med* 2020; **39**: 1459-1462 [PMID: 32198775 DOI: 10.1002/jum.15284]

10 **Yassa M**, Birol P, Mutlu AM, Tekin AB, Sandal K, Tug N. Lung Ultrasound Can Influence the Clinical Treatment of Pregnant Women With COVID-19. *J Ultrasound Med* 2021; **40**: 191-203 [PMID: 32478445 DOI: 10.1002/jum.15367]

11 **Inchingolo R**, Smargiassi A, Mormile F, Marra R, De Carolis S, Lanzone A, Valente S, Corbo GM. Look at the lung: can chest ultrasonography be useful in pregnancy? *Multidiscip Respir Med* 2014; **9**: 32 [PMID: 24936303 DOI: 10.1186/2049-6958-9-32]

12 **Sultan LR**, Sehgal CM. A Review of Early Experience in Lung Ultrasound in the Diagnosis and Management of COVID-19. *Ultrasound Med Biol* 2020; **46**: 2530-2545 [PMID: 32591166 DOI: 10.1016/j.ultrasmedbio.2020.05.012]

13 **Kulkarni S**, Down B, Jha S. Point-of-care lung ultrasound in intensive care during the COVID-19 pandemic. *Clin Radiol* 2020; **75**: 710.e1-710. e4 [PMID: 32405081 DOI: 10.1016/j.crad.2020.05.001]

14 **Buonsenso D**, Pata D, Chiaretti A. COVID-19 outbreak: less stethoscope, more ultrasound. *Lancet Respir Med* 2020; **8**: e27 [PMID: 32203708 DOI: 10.1016/S2213-2600(20)30120-X]

15 **Peixoto AO**, Costa RM, Uzun R. , Fraga AMA, Ribeiro JD, Marson FAL. Applicability of lung ultrasound in COVID-19 diagnosis and evaluation of the disease progression: A systematic review. *Pulmonology* 2021; Online ahead of print [PMID: 33931378 DOI: 10.1016/j.pulmoe.2021.02.004]

16 **Tan G**, Lian X, Zhu Z, Wang Z, Huang F, Zhang Y, Zhao Y, He S, Wang X, Shen H, Lyu G. Use of Lung Ultrasound to Differentiate Coronavirus Disease 2019 (COVID-19) Pneumonia From Community-Acquired Pneumonia. *Ultrasound Med Biol* 2020; **46**: 2651-2658 [PMID: 32622684 DOI: 10.1016/j.ultrasmedbio.2020.05.006]

17 **Volpicelli G**, Gargani L. Sonographic signs and patterns of COVID-19 pneumonia. *Ultrasound J* 2020; **12**: 22 [PMID: 32318891 DOI: 10.1186/s13089-020-00171-w]

18 **Brenner DS**, Liu GY, Omron R, Tang O, Garibaldi BT, Fong TC. Diagnostic accuracy of lung ultrasound for SARS-CoV-2: a retrospective cohort study. *Ultrasound J* 2021; **13**: 12 [PMID: 33644829 DOI: 10.1186/s13089-021-00217-7]

19 **Denina M**, Scolfaro C, Silvestro E, Pruccoli G, Mignone F, Zoppo M, Ramenghi U, Garazzino S. Lung Ultrasound in Children With COVID-19. *Pediatrics* 2020; **146** [PMID: 32317309 DOI: 10.1542/peds.2020-1157]

20 **Wu X**, Sun R, Chen J, Xie Y, Zhang S, Wang X. Radiological findings and clinical characteristics of pregnant women with COVID-19 pneumonia. *Int J Gynaecol Obstet* 2020; **150**: 58-63 [PMID: 32270479 DOI: 10.1002/ijgo.13165]

21 **Sutton D**, Fuchs K, D'Alton M, Goffman D. Universal Screening for SARS-CoV-2 in Women Admitted for Delivery. *N Engl J Med* 2020; **382**: 2163-2164 [PMID: 32283004 DOI: 10.1056/NEJMc2009316]

22 **Vintzileos WS**, Muscat J, Hoffmann E, John NS, Vertichio R, Vintzileos AM, Vo D. Screening all pregnant women admitted to labor and delivery for the virus responsible for coronavirus disease 2019. *Am J Obstet Gynecol* 2020; **223**: 284-286 [PMID: 32348743 DOI: 10.1016/j.ajog.2020.04.024]

23 **Khalil A**, Hill R, Ladhani S, Pattisson K, O'Brien P. Severe acute respiratory syndrome coronavirus 2 in pregnancy: symptomatic pregnant women are only the tip of the iceberg. *Am J Obstet Gynecol* 2020; **223**: 296-297 [PMID: 32387327 DOI: 10.1016/j.ajog.2020.05.005]

24 **Gagliardi L**, Danieli R, Suriano G, Vaccaro A, Tripodi G, Rusconi F, Ramenghi LA. Universal severe acute respiratory syndrome coronavirus 2 testing of pregnant women admitted for delivery in 2 Italian regions. *Am J Obstet Gynecol* 2020; **223**: 291-292 [PMID: 32407787 DOI: 10.1016/j.ajog.2020.05.017]

25 **Li R**, Pei S, Chen B, Song Y, Zhang T, Yang W, Shaman J. Substantial undocumented infection

facilitates the rapid dissemination of novel coronavirus (SARS-CoV-2). *Science* 2020; **368**: 489-493 [PMID: 32179701 DOI: 10.1126/science.abb3221]

26 **Royal College of Obstetrics and Gynaecology**. Principles for the Testing and Triage of Women Seeking Maternity Care in Hospital Settings, During the COVID-19 Pandemic. 2nd ed. [cited 25 January 2021]. Available from: https://www.rcog.org.uk/globalassets/ documents/guidelines/2020-08-10-principles-for-the-testingand-triage-of-women-seeking-maternity-care-in-hospitalsettings-during-the-covid-19-pandemic.pdf

27 **Yassa M**, Yirmibes C, Cavusoglu G, Eksi H, Dogu C, Usta C, Mutlu M, Birol P, Gulumser C, Tug N. Outcomes of universal SARS-CoV-2 testing program in pregnant women admitted to hospital and the adjuvant role of lung ultrasound in screening: a prospective cohort study. *J Matern Fetal Neonatal Med* 2020; **33**: 3820-3826 [PMID: 32691641 DOI: 10.1080/14767058.2020.1798398]

28 **Secco G**, Delorenzo M, Salinaro F, Zattera C, Barcella B, Resta F, Sabena A, Vezzoni G, Bonzano M, Briganti F, Cappa G, Zugnoni F, Demitry L, Mojoli F, Baldanti F, Bruno R, Perlini S; GERICO (Gruppo Esteso RIcerca COronarovirus) Lung US Pavia Study Group. Lung ultrasound presentation of COVID-19 patients: phenotypes and correlations. *Intern Emerg Med* 2021 [PMID: 33646508 DOI: 10.1007/s11739-020-02620-9]

29 **Dargent A**, Chatelain E, Kreitmann L, Quenot JP, Cour M, Argaud L; COVID-LUS study group. Lung ultrasound score to monitor COVID-19 pneumonia progression in patients with ARDS. *PLoS One* 2020; **15**: e0236312 [PMID: 32692769 DOI: 10.1371/journal.pone.0236312]

30 **Buonsenso D**, Raffaelli F, Tamburrini E, Biasucci DG, Salvi S, Smargiassi A, Inchingolo R, Scambia G, Lanzone A, Testa AC, Moro F. Clinical role of lung ultrasound for diagnosis and monitoring of COVID-19 pneumonia in pregnant women. *Ultrasound Obstet Gynecol* 2020; **56**: 106-109 [PMID: 32337795 DOI: 10.1002/uog.22055]

31 **Deng Q**, Cao S, Wang H, Zhang Y, Chen L, Yang Z, Peng Z, Zhou Q. Application of quantitative lung ultrasound instead of CT for monitoring COVID-19 pneumonia in pregnant women: a single-center retrospective study. *BMC Pregnancy Childbirth* 2021; **21**: 259 [PMID: 33771120 DOI: 10.1186/s12884-021-03728-2]

32 **Gil-Rodrigo A**, Llorens-Soriano P, Ramos-Rincón JM. Ultrasound in Pregnant Women With Suspected COVID-19 Infection. *J Ultrasound Med* 2021; **40**: 645-647 [PMID: 32776592 DOI: 10.1002/jum.15419]

33 **Inchingolo R**, Smargiassi A, Moro F, Buonsenso D, Salvi S, Del Giacomo P, Scoppettuolo G, Demi L, Soldati G, Testa AC. The diagnosis of pneumonia in a pregnant woman with coronavirus disease 2019 using maternal lung ultrasound. *Am J Obstet Gynecol* 2020; **223**: 9-11 [PMID: 32360111 DOI: 10.1016/j.ajog.2020.04.020]

34 **Kalafat E**, Yaprak E, Cinar G, Varli B, Ozisik S, Uzun C, Azap A, Koc A. Lung ultrasound and computed tomographic findings in pregnant woman with COVID-19. *Ultrasound Obstet Gynecol* 2020; **55**: 835-837 [PMID: 32249471 DOI: 10.1002/uog.22034]

35 **Porpora MG**, Merlino L, Masciullo L, D'Alisa R, Brandolino G, Galli C, De Luca C, Pecorini F, Fonsi GB, Mingoli A, Franchi C, Oliva A, Manganaro L, Mastroianni CM, Piccioni MG. Does Lung Ultrasound Have a Role in the Clinical Management of Pregnant Women with SARS COV2 Infection? *Int J Environ Res Public Health* 2021; **18** [PMID: 33803223 DOI: 10.3390/ijerph18052762]

36 **Youssef A**, Serra C, Pilu G. Lung ultrasound in the coronavirus disease 2019 pandemic: a practical guide for obstetricians and gynecologists. *Am J Obstet Gynecol* 2020; **223**: 128-131 [PMID: 32437667 DOI: 10.1016/j.ajog.2020.05.014]

37 **Smith MJ**, Hayward SA, Innes SM, Miller ASC. Point-of-care lung ultrasound in patients with COVID-19 - a narrative review. *Anaesthesia* 2020; **75**: 1096-1104 [PMID: 32275766 DOI: 10.1111/anae.15082]

38 **Brainin P**, Claggett B, Lewis EF, Dwyer KH, Merz AA, Silverman MB, Swamy V, Biering-Sørensen T, Rivero J, Cheng S, McMurray JJV, Solomon SD, Platz E. Body mass index and B-lines on lung ultrasonography in chronic and acute heart failure. *ESC Heart Fail* 2020; **7**: 1201-1209 [PMID: 32077268 DOI: 10.1002/ehf2.12640]

39 **Maw AM**, Hassanin A, Ho PM, McInnes MDF, Moss A, Juarez-Colunga E, Soni NJ, Miglioranza MH, Platz E, DeSanto K, Sertich AP, Salame G, Daugherty SL. Diagnostic Accuracy of Point-of-Care Lung Ultrasonography and Chest Radiography in Adults With Symptoms Suggestive of Acute Decompensated Heart Failure: A Systematic Review and Meta-analysis. *JAMA Netw Open* 2019; **2**: e190703 [PMID: 30874784 DOI: 10.1001/jamanetworkopen.2019.0703]

40 **Fox S**, Dugar S. Point-of-care ultrasound and COVID-19. *Cleve Clin J Med* 2020 [PMID: 32409431 DOI: 10.3949/ccjm.87a.ccc019]

41 **Piliego C**, Strumia A, Stone MB, Pascarella G. The Ultrasound-Guided Triage: A New Tool for Prehospital Management of COVID-19 Pandemic. *Anesth Analg* 2020; **131**: e93-e94 [PMID: 32345853 DOI: 10.1213/ANE.0000000000004920]

42 **Dudea SM**. Ultrasonography and SARS-CoV 2 infection: a review of what we know and do not yet know. *Med Ultrason* 2020; **22**: 129-132 [PMID: 32399522 DOI: 10.11152/mu-2612]

Artificial Intelligence in Medical Imaging

Submit a Manuscript: https://www.f6publishing.com

Artif Intell Med Imaging 2021 June 28; 2(3): 64-72

DOI: 10.35711/aimi.v2.i3.64

ISSN 2644-3260 (online)

MINIREVIEWS

Application of radiomics in hepatocellular carcinoma: A review

Zhi-Cheng Jin, Bin-Yan Zhong

ORCID number: Zhi-Cheng Jin 0000-0002-6114-154X; Bin-Yan Zhong 0000-0001-9716-1211.

Author contributions: Jin ZC and Zhong BY contributed to study design, review of literature, interpretation of data, and drafting and revision of the manuscript.

Conflict-of-interest statement: The authors declare that the research was conducted in the absence of any commercial or financial relationships that could be construed as a potential conflict of interest.

Manuscript source: Invited manuscript

Specialty type: Oncology

Country/Territory of origin: China

Zhi-Cheng Jin, Center of Interventional Radiology and Vascular Surgery, Department of Radiology, Zhongda Hospital, Medical School, Southeast University, Nanjing 210009, Jiangsu Province, China

Bin-Yan Zhong, Department of Interventional Radiology, The First Affiliated Hospital of Soochow University, Suzhou 215006, Jiangsu Province, China

Corresponding author: Bin-Yan Zhong, MD, PhD, Doctor, Department of Interventional Radiology, The First Affiliated Hospital of Soochow University, No. 188 Shizi Street, Suzhou 215006, Jiangsu Province, China. byzhongir@sina.com

Abstract

Hepatocellular carcinoma (HCC) is the most common form of primary liver cancer with low 5-year survival rate. The high molecular heterogeneity in HCC poses huge challenges for clinical practice or trial design and has become a major barrier to improving the management of HCC. However, current clinical practice based on single bioptic or archived tumor tissue has been deficient in identifying useful biomarkers. The concept of radiomics was first proposed in 2012 and is different from the traditional imaging analysis based on the qualitative or semi-quantitative analysis by radiologists. Radiomics refers to high-throughput extraction of large amounts number of high-dimensional quantitative features from medical images through machine learning or deep learning algorithms. Using the radiomics method could quantify tumoral phenotypes and heterogeneity, which may provide benefits in clinical decision-making at a lower cost. Here, we review the workflow and application of radiomics in HCC.

Key Words: Hepatocellular carcinoma; Radiomics; Machine learning; Deep learning; Radiogenomics

Core Tip: The high molecular heterogeneity in hepatocellular carcinoma poses huge challenges for clinical practice or trial design and has become a major barrier to improving the management of hepatocellular carcinoma. Radiomics could quantify tumoral phenotypes and heterogeneity, which may provide benefits in clinical decision-making at a lower cost. Here, we review the workflow and application of radiomics in hepatocellular carcinoma.

Peer-review report's scientific quality classification
Grade A (Excellent): 0
Grade B (Very good): 0
Grade C (Good): C
Grade D (Fair): 0
Grade E (Poor): 0

Received: May 13, 2021
Peer-review started: May 13, 2021
First decision: June 2, 2021
Revised: June 19, 2021
Accepted: June 30, 2021
Article in press: June 30, 2021
Published online: June 28, 2021

P-Reviewer: Calabro F
S-Editor: Liu M
L-Editor: Filipodia
P-Editor: Xing YX

Citation: Jin ZC, Zhong BY. Application of radiomics in hepatocellular carcinoma: A review. *Artif Intell Med Imaging* 2021; 2(3): 64-72
URL: https://www.wjgnet.com/2644-3260/full/v2/i3/64.htm
DOI: https://dx.doi.org/10.35711/aimi.v2.i3.64

INTRODUCTION

Liver cancer is one of the most common malignant tumors worldwide. There are approximately 906000 new cases and 830000 deaths every year, ranking as the sixth most commonly diagnosed cancer and the third mortality[1]. Hepatocellular carcinoma (HCC) comprises 75%-85% of cases of primary liver cancer. There is high molecular heterogeneity in HCC at three levels, including the heterogeneity between tumor nodules within the same individual (intertumoral heterogeneity), between different regions of the same tumor nodule (intratumor heterogeneity), and between patients (interpatient heterogeneity)[2]. HCC has one of the fewest somatic mutations in solid tumors that can be targeted by molecular therapies and of which treatment response could not be predicted by mutations in clinical practice[3]. These characteristics of HCC pose huge challenges for clinical practice or trial design and have become a major barrier to improving the management of HCC[4,5]. However, current clinical practice based on single bioptic or archived tumor tissue has been deficient in identifying useful biomarkers[5].

Radiomics was first proposed in 2012 and is different from the traditional imaging analysis based on the qualitative or semi-quantitative analysis by radiologists[6]. This method refers to high-throughput extraction of large amounts of high-dimensional quantitative features from medical images through machine learning (ML) or deep learning (DL) algorithms[7,8]. These features that have been transformed into minable data could be used for diagnosis, treatment evaluation, and prognosis prediction[9]. Using the radiomics method could quantify tumoral phenotypes and heterogeneity, which may provide benefits in clinical decision-making at a lower cost[10,11]. Here, we review the workflow and application of radiomics in HCC.

WORKFLOW OF RADIOMICS

The workflow of radiomics mainly includes: image data acquisition and preprocessing, the volume of interest (VOI) segmentation, feature extraction, model establishment, and performance validation (Figure 1)[9].

Data acquisition

Although radiomics was first and widely utilized in computed tomography (CT) and magnetic resonance imaging (MRI) images, there were more and more studies using ultrasound (US) as well as positron emission tomography images. Most studies were conducted based on retrospective image data sets, even different hospitals and different scanning equipment. The standardized imaging protocols could reduce the unnecessary confounding variability, or it will affect the quality and stability of the extracted imaging features. A previous study found that the feature variability caused by different CT scanners was even comparable to the feature variability found in the tumor[12]. The disclosed imaging protocols were suggested to increase the reproducibility and comparability in future radiomics studies[9].

Segmentation

The three-dimensional VOI segmentation that captures the tumor comprehensive panorama could be delineated by using manual, semi-automatic, and automatic segmentation methods. However, the variability in the segmentation process inevitably introduces bias. Meanwhile, the partial volume effect makes the segmentation challenge that could lead to the blurring of the edge and morphological variation of the lesion. Multiple segmentation is an effective method that can limit bias and help to select robust features, including the evaluation by multiple clinicians and the combination of different segmentation algorithms. However, the commonly used segmentation method in radiomics is manual segmentation and relies on an experienced clinician, which is quite boring and time-consuming. Several semi-automatic or automatic segmentation methods have been reported[13,14]. These

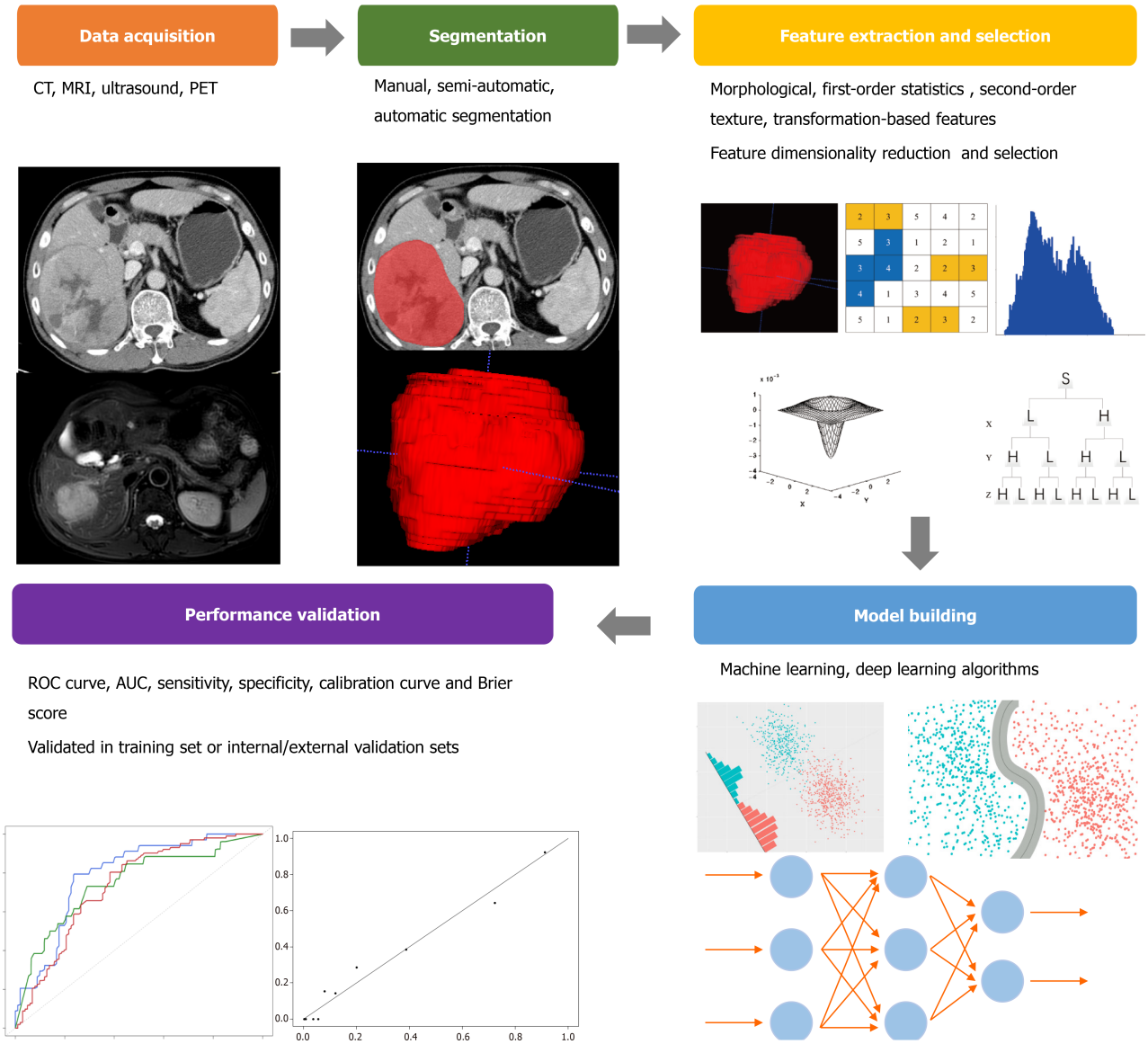

Figure 1 The workflow of radiomics. AUC: Area under the curve; CT: Computed tomography; MRI: Magnetic resonance imaging; PET: Positron emission tomography; ROC: Operating curve.

methods could minimize labor costs and improve the repeatability and reliability of studies but are not widely recognized and applied.

Feature extraction and selection

The high-throughput extraction of quantitative features from VOI is the key process in radiomics analysis after appropriate image preprocessing. The imaging features that are empirically defined by radiologists are named semantic features. These features cannot be described by specific mathematical expressions nor can they be specifically extracted from images, but they are still meaningful in imaging interpretation and clinical application. These non-semantic features quantitatively described by mathematical expressions can usually be divided into four categories: morphological features, first-order statistics features, second-order texture features, and transformation-based features. Morphological features describe the three-dimensional and two- dimensional size and shape of VOI, such as diameter, perimeter, sphericity, and flatness. First-order statistics features (also called histogram features) evaluate the gray-level frequency distribution in VOI, including maximum, median, minimum, and entropy, while second-order texture features are often derived from the gray-level matrix and describe the statistical relationship between voxel gray levels, including gray-level co-occurrence matrix and gray level run length matrix. The voxel gray-level patterns in different spatial frequencies are analyzed by transformation-based features, including Fourier, Gabor, and wavelet features.

According to the number of filters, feature categories, and other parameters, the number of features extracted from the images can be infinite. The inclusion of all relevant features in a predictive model inevitably leads to overfitting, which negatively impacts the efficacy of its prediction performance. It is necessary to introduce a feature selection method to eliminate unsuitable features, that is, feature dimensionality reduction methods (such as principal component analysis or clustering). By reducing redundant and interference items by dimensionality reduction, the features for further analysis contain useful and repeatable information to a large extent.

Model building and performance validation

The prediction model composed of selected features was constructed by an ML algorithm, including support vector machine, random forest, linear discriminant analysis, and so on. The specific method was chosen according to the preference and experience of the researchers. However, different modeling methods have been proved to affect the prediction performance of imaging models and have inherent limitations, such as the independence assumption in logistic regression, feature discretization in Bayesian networks, or network structure dependence in DL. Therefore, a variety of ways could be considered to build the model in the study.

The predictive performance evaluation of the model requires an internal or external validation set to determine whether the model has good generalization performance or only predictability for the specific samples analyzed. This process is often measured by the receiver operating characteristic curve with area under the curve (AUC), sensitivity, and specificity. In addition, the consistency between the observed results and the model prediction was also evaluated necessarily, which can be evaluated by the calibration curve and Brier score. An effective model shows consistency in both training and validation sets. The models validated by an independent external set are more reliable than those validated by an internal set, and of course, the models that could be prospectively verified are more persuasive.

THE APPLICATION OF RADIOMICS IN HCC

Diagnosis

Imaging is a crucial part of the HCC diagnosis. Multiphasic contrast-enhanced CT or contrast-enhanced MRI should be used first with high sensitivity recommended by the European Association for the Study of the Liver[15]. Li *et al*[16] extracted the texture features from the SPAIR T2WI sequence in MRI and used four different classifiers to identify single intrahepatic lesions (hepatic hemangioma, hepatic metastases, and HCC). The error rates were 11.7% (hepatic hemangioma *vs* hepatic metastases), 9.6% (hepatic metastases *vs* HCC), and 9.7% (hepatic hemangioma *vs* HCC). The combination of quantitative apparent diffusion coefficient histogram parameters and the Liver Imaging Reporting And Data System could distinguish HCC from other subtypes of primary liver cancer, such as intrahepatic cholangiocarcinoma and mixed HCC-intrahepatic cholangiocarcinoma[17]. A total of 63 patients confirmed by pathology were included, and it was found that the model combined with gender, Liver Imaging Reporting And Data System, and the fifth percentile apparent diffusion coefficient could achieve a good prediction efficiency. The AUCs could reach 0.90/0.89 with the accuracy of 81.5%/80.0%, the sensitivity of 79.3%/86.2%, and the specificity of 88.9%/77.8% for two independent observers. Huang *et al*[18] managed to distinguish dual phenotypic HCC by different classifiers based on Gd-EOB-DTPA-enhanced MRI and showed good predictive performance.

For the new HCC nodules in patients with a liver cirrhosis background, radiomics features extracted from multiphasic contrast-enhanced CT combined with the ML algorithm could bring benefits. Mokrane *et al*[19] retrospectively included 178 patients from 27 centers and divided them into a training set (142 patients) and validation set (36 patients). All the patients had nodules that were classified as indeterminate liver nodules by the European Association for the Study of the Liver guidelines, and the histological classification was finally confirmed by liver biopsy. A total of 13920 quantitative radiomics features were extracted from the plain, arterial, venous, and dual-phase (delta) phases. Three supervised ML classification algorithms: K nearest neighbor, support vector machine, and random forest algorithm were used to establish the models. A single feature was finally obtained, which represented the characteristics of changes in nodule phenotype between arterial and portal venous phases (corresponds to the "washout" pattern during the contrast agent clearance). Finally,

the radiomics signature used reached an AUC value of 0.66 with a sensitivity of 0.70 and specificity of 0.59 in the external validation set.

US is one of the important methods in the diagnostic algorithm and recall policy by the European Association for the Study of the Liver guidelines[15]. However, US images are more heterogeneous because of the images acquired by different clinicians with multiple examination parameters. There was a study that reported that the features extracted from US images could be classified by using neural network classifiers to distinguish focal liver lesions, including typical and atypical cysts, hepatic hemangiomas, liver metastases, and HCC lesions, with an accuracy of up to 95%[20]. A multitask DL algorithm was constructed that detects and characterizes focal liver lesions in a public dataset[21]. The model simultaneously yielded AUCs of 0.935 for lesion detection and 0.916 for focal liver lesions characterization (benign *vs* malignant).

Radiomics could effectively diagnose and distinguish the HCC lesion from the different intrahepatic lesions, new nodules, and even the subtypes of primary liver cancer. Although the above studies are based on different imaging modalities and ML/DL methods, this method is expected to further assist doctors in clinical diagnosis and decision-making in the future.

Treatment evaluation

Surgical resection is the first choice for HCC patients with good performance status and liver function reserve. But the postoperative 5-year recurrence rate could be as high as 70%. To solve this problem, a multicenter retrospective study was carried out from three independent centers. The study included 295 early-stage HCC patients within Milan criteria who have received preoperative contrast-enhanced CT examination. Recurrence-free survival was selected as the primary endpoint of this study. Based on 177 patients from one center (training set), two prediction models have been constructed that incorporated preoperative variables or postoperative variables. The results showed that the prediction efficiency of the two radiomics-based models was higher than that of previous clinical models and staging systems and can well stratify patients with a low, moderate, and high risk of recurrence.

The application of radiomics in predicting postoperative recurrence has also been verified in other studies. In addition, some studies have found that the radiomics model based on preoperative MRI images can better predict the 5-year survival of patients after hepatectomy. Cai *et al*[22] retrospectively included 112 patients who underwent hepatectomy to predict postoperative liver failure by a radiomics-based nomogram. The AUC value of the training set was 0.822 (95% confidence interval: 0.753-0.917), and the AUC value of the validation set was 0.762 (95% confidence interval: 0.576-0.948). When it was compared with MELD, Child-Pugh, and ALBI score, the radiomics model showed a significant advantage. The researchers conducted a prospective validation analysis of 13 patients who underwent hepatectomy with an AUC of 0.833 (95% confidence interval: 0.591-1.000). Decision curve analysis showed that the model could bring clinical benefits. Radiomic features could identify the tumor invasion and predict recurrence after liver transplantation[23].

Ablation is recommended for HCC patients with Barcelona Clinic Liver Cancer 0 or A stage who are not suitable for surgery. Radiomic features extracted from perioperative CT images could predict early recurrence after curative ablation[24,25]. Among them, the features based on portal vein phase CT images performed best in the validation set. When the clinicopathological factors were added to the model, the portal vein phase-based combined model showed good prediction performance in the training/validation set and significantly better than that of the simple clinical model. Microwave ablation was performed in pigs under CT guidance for improving the visualization of post ablational coagulation necrosis in a proof of concept study[26]. The results showed that radiomic profiles of the fully necrotic areas seemed to be different from those areas with vital tissue. The subregion radiomics analysis could identify these differences with classification algorithms.

Transarterial chemoembolization (TACE) is the most widely used treatment for unresectable HCC in clinical practice. Radiomics plays a role in the prediction of treatment response to TACE[27-29]. Chen *et al*[27] analyzed the radiomic features extracted from tumoral VOI and peritumoral VOI, drawn at the hepatic arterial and non-contrast phases, respectively. The radiomic signature extracted from the peritumoral VOI with expanded 10 mm rim away from the main tumor part achieved excellent performance in predicting the first TACE response. Several studies established a radiomic model based on the preoperative images to predict long-term outcomes of patients who underwent TACE with good performance[30,31]. However, there were various confounding factors during multiple TACE sessions that may weaken the actual predictive performance. Fu *et al*[32] included 520 patients from five

independent centers (divided into a training set and validation set). A comprehensive model including treatment (liver resection or TACE), age, sex, modified Barcelona Clinic Liver Cancer stage, fusion focus, tumor capsule, and three radiomic features was established with good differentiation and calibration. The AUC value of the predicted 3-year recurrence-free survival was 0.80 in the training set and 0.75 in the test set.

Sorafenib is the first oral multikinase inhibitor recommended in patients with advanced HCC. Various clinical trials tried to explore the possibility of combining sorafenib and TACE that may inhibit revascularization and tumor proliferation after TACE. Most of these trials failed, except the TACTICS trial conducted recently. It is important to identify HCC patients who may benefit from the combination of TACE plus sorafenib. A DL-based radiomic model provided a significant prediction value with an AUC value of 0.717 in the training set and 0.714 in the validation set[33].

Radiopathologic evaluation

Microvascular invasion (MVI) of HCC mainly refers to the presence of cancer cells in the endothelial-lined vascular lumen under the microscope, which is a powerful validated, important independent risk factor for early recurrence and poor survival after surgical resection of HCC. Radiomic features extracted from preoperative enhanced MRI multi-phase images could predict the occurrence of MVI favorably[34,35]. By using the least absolute shrinkage and selection operator method to select appropriate radiomic features, the predictive performance of the combined model incorporating clinicoradiological predictors and radiomic features was better than the clinicoradiological model (AUC 0.943 *vs* 0.850 in the training set, and 0.861 *vs* 0.759 in the validation set). The sensitivity, specificity, and accuracy of the combined model were 88.2%/89.5%, 87.5%/81.4%, and 87.7%/83.9% in two sets, respectively. Several studies reported that using contrast-enhanced CT images to develop and validate radiomics nomogram was a clinically useful tool to identify patients[36,37]. However, a retrospective study that included 495 patients with postoperative MVI status confirmed by histology (MVI- group, n = 346, and MVI + group, n = 149)[38] found that radiomics analysis with current CT imaging protocols does not provide significant additional value to the conventional semantic features.

Pathological grading of HCC is one of the factors that influence prognosis. Most patients with high-grade tumors have a higher rate of intrahepatic recurrence than those without low-grade tumors. The radiomics signatures based on MRI T1WI or T2WI images could be helpful for the preoperative prediction of the pathological grade of HCC[39]. The combination of the radiomic signatures and clinical factors achieved the best predictive performance over the other simple model and distinguished between high-grade and low-grade HCC (AUC = 0.800). In addition, cytokeratin 19 status of HCC that is associated with clinical aggressiveness could be identified by a radiomic-based model with satisfactory prediction performance[40]. Ye *et al*[41] managed to use the texture feature analysis on gadoxetic acid-enhanced MRI images preoperatively to predict Ki-67 status of HCC. However, the optimal cut-off value of the Ki-67 level was defined by the researcher, which weakened the generalization of the study.

Radiogenomics

Gene expression patterns of cancer tissues could reflect the underlying cellular pathophysiology and enrich the understanding of cellular pathways and numerous pathological conditions. Imaging traits have the potential to be a surrogate marker of the clinically relevant genomic/molecular signature of HCC[42-45]. One study found that the dynamic imaging traits from CT systematically correlated with the global gene expression programs of HCC[42]. The combination of 28 imaging traits was sufficient to reconstruct the variation of 116 gene expression profiles, revealing cell proliferation, liver synthetic function, and patient prognosis. Moreover, they developed a two-imaging-trait decision tree, including internal arteries and hypodense halos in HCC that is associated with a gene expression signature of venous invasion and could predict histologic venous invasion and survival of patients. Based on that result, a similar team defined a contrast-enhanced CT imaging biomarker for predicting MVI named radiogenomic venous invasion[43]. In a multicenter retrospective study, the radiogenomic venous invasion biomarker was a robust predictor of MVI with a diagnostic accuracy of 89%, sensitivity of 76%, and specificity of 94% and was associated with a poor overall survival that could have broad clinical use. They considered that radiogenomic venous invasion derived from a gene expression signature of venous invasion may reflect a more fundamental phenotype of the tumor.

Qualitative and quantitative MRI radiomic features could serve as the noninvasive biomarker to predict HCC immuno-oncological characteristics and tumor recurrence [46]. One study analyzed the correlation between radiomics, immunoprofiling (CD3, CD68, CD31), and genomic (PD-1 at the protein level, *PD-L1* and *CTLA4* at the mRNA expression level) features with statistical significance[46]. Radiomic features, including tumor size, showed good prediction performance for early HCC recurrence after resection, while immunoprofiling and genomic features did not.

CONCLUSION

Systemic therapy in advanced HCC has developed rapidly in recent years, with the most prominent success of the combination of atezolizumab (anti-PD-L1 antibody) and bevacizumab (anti-VEGF antibody). However, due to the huge tumor heterogeneity in HCC, several promising trials (such as keynote-240 and checkmate-459) have failed, and the best objective response rates of successful systemic therapies are only around 30%. In addition, there are more and more ongoing trials in the adjuvant or combination therapies setting of HCC that are explored and practiced currently. Personalized treatment and more precise patient stratification may be required under such circumstances. Radiomics technology based on ML/DL algorithms is expected to become a bridge that connects the clinical personalized precision treatment of HCC patients and its tumor phenotype. Further radiomics research with multicenter and prospective validation is still needed for improving its interpretability and reproducibility.

REFERENCES

1 **Sung H**, Ferlay J, Siegel RL, Laversanne M, Soerjomataram I, Jemal A, Bray F. Global Cancer Statistics 2020: GLOBOCAN Estimates of Incidence and Mortality Worldwide for 36 Cancers in 185 Countries. *CA Cancer J Clin* 2021; **71**: 209-249 [PMID: 33538338 DOI: 10.3322/caac.21660]

2 **Craig AJ**, von Felden J, Garcia-Lezana T, Sarcognato S, Villanueva A. Tumour evolution in hepatocellular carcinoma. *Nat Rev Gastroenterol Hepatol* 2020; **17**: 139-152 [PMID: 31792430 DOI: 10.1038/s41575-019-0229-4]

3 **Villanueva A**. Hepatocellular Carcinoma. *N Engl J Med* 2019; **380**: 1450-1462 [PMID: 30970190 DOI: 10.1056/NEJMra1713263]

4 **Lin DC**, Mayakonda A, Dinh HQ, Huang P, Lin L, Liu X, Ding LW, Wang J, Berman BP, Song EW, Yin D, Koeffler HP. Genomic and Epigenomic Heterogeneity of Hepatocellular Carcinoma. *Cancer Res* 2017; **77**: 2255-2265 [PMID: 28302680 DOI: 10.1158/0008-5472.CAN-16-2822]

5 **Lu LC**, Hsu CH, Hsu C, Cheng AL. Tumor Heterogeneity in Hepatocellular Carcinoma: Facing the Challenges. *Liver Cancer* 2016; **5**: 128-138 [PMID: 27386431 DOI: 10.1159/000367754]

6 **Lambin P**, Rios-Velazquez E, Leijenaar R, Carvalho S, van Stiphout RG, Granton P, Zegers CM, Gillies R, Boellard R, Dekker A, Aerts HJ. Radiomics: extracting more information from medical images using advanced feature analysis. *Eur J Cancer* 2012; **48**: 441-446 [PMID: 22257792 DOI: 10.1016/j.ejca.2011.11.036]

7 **Piccialli F**, Calabrò F, Crisci D, Cuomo S, Prezioso E, Mandile R, Troncone R, Greco L, Auricchio R. Precision medicine and machine learning towards the prediction of the outcome of potential celiac disease. *Sci Rep* 2021; **11**: 5683 [PMID: 33707543 DOI: 10.1038/s41598-021-84951-x]

8 **Piccialli F**, Somma VD, Giampaolo F, Cuomo S, Fortino G. A survey on deep learning in medicine: Why, how and when? *Information Fusion* 2021; **66**: 111-137 [DOI: 10.1016/j.inffus.2020.09.006]

9 **Lambin P**, Leijenaar RTH, Deist TM, Peerlings J, de Jong EEC, van Timmeren J, Sanduleanu S, Larue RTHM, Even AJG, Jochems A, van Wijk Y, Woodruff H, van Soest J, Lustberg T, Roelofs E, van Elmpt W, Dekker A, Mottaghy FM, Wildberger JE, Walsh S. Radiomics: the bridge between medical imaging and personalized medicine. *Nat Rev Clin Oncol* 2017; **14**: 749-762 [PMID: 28975929 DOI: 10.1038/nrclinonc.2017.141]

10 **Aerts HJ**, Velazquez ER, Leijenaar RT, Parmar C, Grossmann P, Carvalho S, Bussink J, Monshouwer R, Haibe-Kains B, Rietveld D, Hoebers F, Rietbergen MM, Leemans CR, Dekker A, Quackenbush J, Gillies RJ, Lambin P. Decoding tumour phenotype by noninvasive imaging using a quantitative radiomics approach. *Nat Commun* 2014; **5**: 4006 [PMID: 24892406 DOI: 10.1038/ncomms5006]

11 **O'Connor JP**, Rose CJ, Waterton JC, Carano RA, Parker GJ, Jackson A. Imaging intratumor heterogeneity: role in therapy response, resistance, and clinical outcome. *Clin Cancer Res* 2015; **21**: 249-257 [PMID: 25421725 DOI: 10.1158/1078-0432.CCR-14-0990]

12 **Mackin D**, Fave X, Zhang LF, Fried D, Yang JZ, Taylor B, Rodriguez-Rivera E, Dodge C, Jones AK, Court L. Measuring Computed Tomography Scanner Variability of Radiomics Features. *Invest Radiol* 2015; **50**: 757-765 [PMID: 26115366 DOI: 10.1097/rli.0000000000000180]

13 **Heye T**, Merkle EM, Reiner CS, Davenport MS, Horvath JJ, Feuerlein S, Breault SR, Gall P, Bashir MR, Dale BM, Kiraly AP, Boll DT. Reproducibility of dynamic contrast-enhanced MR imaging. Part II. Comparison of intra- and interobserver variability with manual region of interest placement versus semiautomatic lesion segmentation and histogram analysis. *Radiology* 2013; **266**: 812-821 [PMID: 23220891 DOI: 10.1148/radiol.12120255]

14 **Parmar C**, Rios Velazquez E, Leijenaar R, Jermoumi M, Carvalho S, Mak RH, Mitra S, Shankar BU, Kikinis R, Haibe-Kains B, Lambin P, Aerts HJ. Robust Radiomics feature quantification using semiautomatic volumetric segmentation. *PLoS One* 2014; **9**: e102107 [PMID: 25025374 DOI: 10.1371/journal.pone.0102107]

15 **European Association for the Study of the Liver**. EASL Clinical Practice Guidelines: Management of hepatocellular carcinoma. *J Hepatol* 2018; **69**: 182-236 [PMID: 29628281 DOI: 10.1016/j.jhep.2018.03.019]

16 **Li Z**, Mao Y, Huang W, Li H, Zhu J, Li W, Li B. Texture-based classification of different single liver lesion based on SPAIR T2W MRI images. *BMC Med Imaging* 2017; **17**: 42 [PMID: 28705145 DOI: 10.1186/s12880-017-0212-x]

17 **Lewis S**, Peti S, Hectors SJ, King M, Rosen A, Kamath A, Putra J, Thung S, Taouli B. Volumetric quantitative histogram analysis using diffusion-weighted magnetic resonance imaging to differentiate HCC from other primary liver cancers. *Abdom Radiol (NY)* 2019; **44**: 912-922 [PMID: 30712136 DOI: 10.1007/s00261-019-01906-7]

18 **Huang X**, Long L, Wei J, Li Y, Xia Y, Zuo P, Chai X. Radiomics for diagnosis of dual-phenotype hepatocellular carcinoma using Gd-EOB-DTPA-enhanced MRI and patient prognosis. *J Cancer Res Clin Oncol* 2019; **145**: 2995-3003 [PMID: 31664520 DOI: 10.1007/s00432-019-03062-3]

19 **Mokrane FZ**, Lu L, Vavasseur A, Otal P, Peron JM, Luk L, Yang H, Ammari S, Saenger Y, Rousseau H, Zhao B, Schwartz LH, Dercle L. Radiomics machine-learning signature for diagnosis of hepatocellular carcinoma in cirrhotic patients with indeterminate liver nodules. *Eur Radiol* 2020; **30**: 558-570 [PMID: 31444598 DOI: 10.1007/s00330-019-06347-w]

20 **Virmani J**, Kumar V, Kalra N, Khandelwal N. Neural network ensemble based CAD system for focal liver lesions from B-mode ultrasound. *J Digit Imaging* 2014; **27**: 520-537 [PMID: 24687642 DOI: 10.1007/s10278-014-9685-0]

21 **Schmauch B**, Herent P, Jehanno P, Dehaene O, Saillard C, Aubé C, Luciani A, Lassau N, Jégou S. Diagnosis of focal liver lesions from ultrasound using deep learning. *Diagn Interv Imaging* 2019; **100**: 227-233 [PMID: 30926443 DOI: 10.1016/j.diii.2019.02.009]

22 **Cai W**, He B, Hu M, Zhang W, Xiao D, Yu H, Song Q, Xiang N, Yang J, He S, Huang Y, Huang W, Jia F, Fang C. A radiomics-based nomogram for the preoperative prediction of posthepatectomy liver failure in patients with hepatocellular carcinoma. *Surg Oncol* 2019; **28**: 78-85 [PMID: 30851917 DOI: 10.1016/j.suronc.2018.11.013]

23 **Guo D**, Gu D, Wang H, Wei J, Wang Z, Hao X, Ji Q, Cao S, Song Z, Jiang J, Shen Z, Tian J, Zheng H. Radiomics analysis enables recurrence prediction for hepatocellular carcinoma after liver transplantation. *Eur J Radiol* 2019; **117**: 33-40 [PMID: 31307650 DOI: 10.1016/j.ejrad.2019.05.010]

24 **Yuan C**, Wang Z, Gu D, Tian J, Zhao P, Wei J, Yang X, Hao X, Dong D, He N, Sun Y, Gao W, Feng J. Prediction early recurrence of hepatocellular carcinoma eligible for curative ablation using a Radiomics nomogram. *Cancer Imaging* 2019; **19**: 21 [PMID: 31027510 DOI: 10.1186/s40644-019-0207-7]

25 **Shan QY**, Hu HT, Feng ST, Peng ZP, Chen SL, Zhou Q, Li X, Xie XY, Lu MD, Wang W, Kuang M. CT-based peritumoral radiomics signatures to predict early recurrence in hepatocellular carcinoma after curative tumor resection or ablation. *Cancer Imaging* 2019; **19**: 11 [PMID: 30813956 DOI: 10.1186/s40644-019-0197-5]

26 **Bressem KK**, Adams LC, Vahldiek JL, Erxleben C, Poch F, Lehmann KS, Hamm B, Niehues SM. Subregion Radiomics Analysis to Display Necrosis After Hepatic Microwave Ablation-A Proof of Concept Study. *Invest Radiol* 2020; **55**: 422-429 [PMID: 32028297 DOI: 10.1097/RLI.0000000000000653]

27 **Chen M**, Cao J, Hu J, Topatana W, Li S, Juengpanich S, Lin J, Tong C, Shen J, Zhang B, Wu J, Pocha C, Kudo M, Amedei A, Trevisani F, Sung PS, Zaydfudim VM, Kanda T, Cai X. Clinical-Radiomic Analysis for Pretreatment Prediction of Objective Response to First Transarterial Chemoembolization in Hepatocellular Carcinoma. *Liver Cancer* 2021; **10**: 38-51 [PMID: 33708638 DOI: 10.1159/000512028]

28 **Park HJ**, Kim JH, Choi SY, Lee ES, Park SJ, Byun JY, Choi BI. Prediction of Therapeutic Response of Hepatocellular Carcinoma to Transcatheter Arterial Chemoembolization Based on Pretherapeutic Dynamic CT and Textural Findings. *AJR Am J Roentgenol* 2017; **209**: W211-W220 [PMID: 28813195 DOI: 10.2214/AJR.16.17398]

29 **Jin Z**, Chen L, Zhong B, Zhou H, Zhu H, Song J, Guo J, Zhu X, Ji J, Ni C, Teng G. Machine-learning analysis of contrast-enhanced computed tomography radiomics predicts patients with hepatocellular carcinoma who are unsuitable for initial transarterial chemoembolization monotherapy: A multicenter study. *Transl Oncol* 2021; **14**: 101034 [PMID: 33567388 DOI: 10.1016/j.tranon.2021.101034]

30 **Kong C**, Zhao Z, Chen W, Lv X, Shu G, Ye M, Song J, Ying X, Weng Q, Weng W, Fang S, Chen M, Tu J, Ji J. Prediction of tumor response *via* a pretreatment MRI radiomics-based nomogram in HCC treated with TACE. *Eur Radiol*2021 epub ahead of print [PMID: 33860832 DOI: 10.1007/s00330-021-07910-0]

31 **Zhao Y**, Wang N, Wu J, Zhang Q, Lin T, Yao Y, Chen Z, Wang M, Sheng L, Liu J, Song Q, Wang F,

An X, Guo Y, Li X, Wu T, Liu AL. Radiomics Analysis Based on Contrast-Enhanced MRI for Prediction of Therapeutic Response to Transarterial Chemoembolization in Hepatocellular Carcinoma. *Front Oncol* 2021; **11**: 582788 [PMID: 33868988 DOI: 10.3389/fonc.2021.582788]

32 **Fu S**, Wei J, Zhang J, Dong D, Song J, Li Y, Duan C, Zhang S, Li X, Gu D, Chen X, Hao X, He X, Yan J, Liu Z, Tian J, Lu L. Selection Between Liver Resection Versus Transarterial Chemoembolization in Hepatocellular Carcinoma: A Multicenter Study. *Clin Transl Gastroenterol* 2019; **10**: e00070 [PMID: 31373932 DOI: 10.14309/ctg.0000000000000070]

33 **Zhang L**, Xia W, Yan ZP, Sun JH, Zhong BY, Hou ZH, Yang MJ, Zhou GH, Wang WS, Zhao XY, Jian JM, Huang P, Zhang R, Zhang S, Zhang JY, Li Z, Zhu XL, Gao X, Ni CF. Deep Learning Predicts Overall Survival of Patients With Unresectable Hepatocellular Carcinoma Treated by Transarterial Chemoembolization Plus Sorafenib. *Front Oncol* 2020; **10**: 593292 [PMID: 33102242 DOI: 10.3389/fonc.2020.593292]

34 **Yang L**, Gu D, Wei J, Yang C, Rao S, Wang W, Chen C, Ding Y, Tian J, Zeng M. A Radiomics Nomogram for Preoperative Prediction of Microvascular Invasion in Hepatocellular Carcinoma. *Liver Cancer* 2019; **8**: 373-386 [PMID: 31768346 DOI: 10.1159/000494099]

35 **Song D**, Wang Y, Wang W, Cai J, Zhu K, Lv M, Gao Q, Zhou J, Fan J, Rao S, Wang M, Wang X. Using deep learning to predict microvascular invasion in hepatocellular carcinoma based on dynamic contrast-enhanced MRI combined with clinical parameters. *J Cancer Res Clin Oncol*2021 epub ahead of print [PMID: 33839938 DOI: 10.1007/s00432-021-03617-3]

36 **Ma X**, Wei J, Gu D, Zhu Y, Feng B, Liang M, Wang S, Zhao X, Tian J. Preoperative radiomics nomogram for microvascular invasion prediction in hepatocellular carcinoma using contrast-enhanced CT. *Eur Radiol* 2019; **29**: 3595-3605 [PMID: 30770969 DOI: 10.1007/s00330-018-5985-y]

37 **Ni M**, Zhou X, Lv Q, Li Z, Gao Y, Tan Y, Liu J, Liu F, Yu H, Jiao L, Wang G. Radiomics models for diagnosing microvascular invasion in hepatocellular carcinoma: which model is the best model? *Cancer Imaging* 2019; **19**: 60 [PMID: 31455432 DOI: 10.1186/s40644-019-0249-x]

38 **Xu X**, Zhang HL, Liu QP, Sun SW, Zhang J, Zhu FP, Yang G, Yan X, Zhang YD, Liu XS. Radiomic analysis of contrast-enhanced CT predicts microvascular invasion and outcome in hepatocellular carcinoma. *J Hepatol* 2019; **70**: 1133-1144 [PMID: 30876945 DOI: 10.1016/j.jhep.2019.02.023]

39 **Wu M**, Tan H, Gao F, Hai J, Ning P, Chen J, Zhu S, Wang M, Dou S, Shi D. Predicting the grade of hepatocellular carcinoma based on non-contrast-enhanced MRI radiomics signature. *Eur Radiol* 2019; **29**: 2802-2811 [PMID: 30406313 DOI: 10.1007/s00330-018-5787-2]

40 **Wang W**, Gu D, Wei J, Ding Y, Yang L, Zhu K, Luo R, Rao SX, Tian J, Zeng M. A radiomics-based biomarker for cytokeratin 19 status of hepatocellular carcinoma with gadoxetic acid-enhanced MRI. *Eur Radiol* 2020; **30**: 3004-3014 [PMID: 32002645 DOI: 10.1007/s00330-019-06585-y]

41 **Ye Z**, Jiang H, Chen J, Liu X, Wei Y, Xia C, Duan T, Cao L, Zhang Z, Song B. Texture analysis on gadoxetic acid enhanced-MRI for predicting Ki-67 status in hepatocellular carcinoma: A prospective study. *Chin J Cancer Res* 2019; **31**: 806-817 [PMID: 31814684 DOI: 10.21147/j.issn.1000-9604.2019.05.10]

42 **Segal E**, Sirlin CB, Ooi C, Adler AS, Gollub J, Chen X, Chan BK, Matcuk GR, Barry CT, Chang HY, Kuo MD. Decoding global gene expression programs in liver cancer by noninvasive imaging. *Nat Biotechnol* 2007; **25**: 675-680 [PMID: 17515910 DOI: 10.1038/nbt1306]

43 **Banerjee S**, Wang DS, Kim HJ, Sirlin CB, Chan MG, Korn RL, Rutman AM, Siripongsakun S, Lu D, Imanbayev G, Kuo MD. A computed tomography radiogenomic biomarker predicts microvascular invasion and clinical outcomes in hepatocellular carcinoma. *Hepatology* 2015; **62**: 792-800 [PMID: 25930992 DOI: 10.1002/hep.27877]

44 **Taouli B**, Hoshida Y, Kakite S, Chen X, Tan PS, Sun X, Kihira S, Kojima K, Toffanin S, Fiel MI, Hirschfield H, Wagner M, Llovet JM. Imaging-based surrogate markers of transcriptome subclasses and signatures in hepatocellular carcinoma: preliminary results. *Eur Radiol* 2017; **27**: 4472-4481 [PMID: 28439654 DOI: 10.1007/s00330-017-4844-6]

45 **Xia W**, Chen Y, Zhang R, Yan Z, Zhou X, Zhang B, Gao X. Radiogenomics of hepatocellular carcinoma: multiregion analysis-based identification of prognostic imaging biomarkers by integrating gene data-a preliminary study. *Phys Med Biol* 2018; **63**: 035044 [PMID: 29311419 DOI: 10.1088/1361-6560/aaa609]

46 **Hectors SJ**, Lewis S, Besa C, King MJ, Said D, Putra J, Ward S, Higashi T, Thung S, Yao S, Laface I, Schwartz M, Gnjatic S, Merad M, Hoshida Y, Taouli B. MRI radiomics features predict immuno-oncological characteristics of hepatocellular carcinoma. *Eur Radiol* 2020; **30**: 3759-3769 [PMID: 32086577 DOI: 10.1007/s00330-020-06675-2]

Artificial Intelligence in Medical Imaging

Submit a Manuscript: https://www.f6publishing.com

Artif Intell Med Imaging 2021 June 28; 2(3): 73-85

DOI: 10.35711/aimi.v2.i3.73

ISSN 2644-3260 (online)

MINIREVIEWS

Artificial intelligence in coronary computed tomography angiography

Zhe-Zhe Zhang, Yan Guo, Yang Hou

ORCID number: Zhe-Zhe Zhang 0000-0002-4947-8270; Yan Guo 0000-0002-0565-640X; Yang Hou 0000-0002-9184-5441.

Author contributions: Zhang ZZ performed the majority of literature search and manuscript revision, and prepared the figures and tables; Guo Y performed data acquisition and coordinated the writing; Hou Y read and approved the final manuscript.

Supported by the National Natural Science Foundation of China, No. 82071920 and No. 81901741; and the Key Research & Development Plan of Liaoning Province, No. 2020JH2/10300037.

Conflict-of-interest statement: There is no conflict of interest associated with any of the senior author or other coauthors who contributed their efforts in this manuscript.

Zhe-Zhe Zhang, Yang Hou, Department of Radiology, Shengjing Hospital of China Medical University, Shenyang 110004, Liaoning Province, China

Yan Guo, GE Healthcare, Beijing 100176, China

Corresponding author: Yang Hou, PhD, Professor, Department of Radiology, Shengjing Hospital of China Medical University, No. 36 Sanhao Street, Heping District, Shenyang 110004, Liaoning Province, China. houyang1973@163.com

Abstract

Coronary computed tomography angiography (CCTA) is recommended as a frontline diagnostic tool in the non-invasive assessment of patients with suspected coronary artery disease (CAD) and cardiovascular risk stratification. To date, artificial intelligence (AI) techniques have brought major changes in the way that we make individualized decisions for patients with CAD. Applications of AI in CCTA have produced improvements in many aspects, including assessment of stenosis degree, determination of plaque type, identification of high-risk plaque, quantification of coronary artery calcium score, diagnosis of myocardial infarction, estimation of computed tomography-derived fractional flow reserve, left ventricular myocardium analysis, perivascular adipose tissue analysis, prognosis of CAD, and so on. The purpose of this review is to provide a comprehensive overview of current status of AI in CCTA.

Key Words: Coronary computed tomography angiography; Coronary artery disease; Artificial intelligence; Deep learning; Machine learning; Prognosis

Core Tip: The application of artificial intelligence in coronary computed tomography angiography mainly focuses on the following aspects: (1) Studies based on the coronary arteries and plaques for determination of stenosis degree, identification of plaque types, quantification of coronary artery calcium score, prediction of myocardial infarction, and prognosis evaluation; (2) Studies around the perivascular adipose tissue, which were mainly conducted using radiomics analysis and machine learning algorithm, for improvement of risk stratification; and (3) Studies based on the texture analysis of the left ventricular myocardium for assessment of functionally significant stenosis or for prognosis evaluation.

Manuscript source: Invited manuscript

Specialty type: Medical laboratory technology

Country/Territory of origin: China

Peer-review report's scientific quality classification

Grade A (Excellent): 0
Grade B (Very good): B
Grade C (Good): C
Grade D (Fair): 0
Grade E (Poor): 0

Received: May 22, 2021
Peer-review started: May 22, 2021
First decision: June 16, 2021
Revised: June 20, 2021
Accepted: July 2, 2021
Article in press: July 2, 2021
Published online: June 28, 2021

P-Reviewer: Kosuga T, Tanabe S
S-Editor: Liu M
L-Editor: Wang TQ
P-Editor: Xing YX

Citation: Zhang ZZ, Guo Y, Hou Y. Artificial intelligence in coronary computed tomography angiography. *Artif Intell Med Imaging* 2021; 2(3): 73-85
URL: https://www.wjgnet.com/2644-3260/full/v2/i3/73.htm
DOI: https://dx.doi.org/10.35711/aimi.v2.i3.73

INTRODUCTION

Coronary computed tomography angiography (CCTA) has merged as a first-line diagnostic tool in the non-invasive evaluation of patients with suspected coronary artery disease (CAD), as recommended in the international guidelines[1,2]. With rich information provided in the luminal stenosis, the morphology and composition of plaques, and the overall circulation, CCTA can safely rule out the obstructive CAD and improve prognosis.

However, the information derived from CCTA images is recognized and interpreted by human readers, and varies among different scanning protocols, scanners, contrast medium injection protocols, and readers. The arrival of artificial intelligence (AI) brought hope that it can be applied for intelligent decision-making with autonomous acquired knowledge by identifying and extracting patterns among a group of observations[3,4].

With the frontline role of CCTA in the diagnostic strategies for CAD, "big data" is available and offers an optimal platform to bridge AI with CCTA. Recently, AI techniques in CCTA have gained much attention and have been widely applied in clinical care ranging from diagnosis to prognostic stratification. We seek to summarize the recent application of AI techniques in CCTA images, so as to investigate and identify the most important and promising research topics, the problems that have been resolved and remain to be resolved, and the future directions with many challenges and opportunities.

CURRENT APPLICATION OF AI IN CCTA

The application of AI in CCTA images mainly focuses on the following aspects: (1) Studies based on the coronary arteries and plaques for determination of stenosis degree, identification of plaque types, quantification of coronary artery calcium (CAC) score, prediction of myocardial infarction (MI), and prognosis evaluation; (2) studies around the perivascular adipose tissue (PVAT), which were mainly conducted using radiomics analysis and machine learning (ML) algorithm, for improvement of risk stratification; and (3) studies based on the texture analysis of the left ventricular myocardium (LVM) for assessment of functionally significant stenosis or for prognosis evaluation, as shown in Figure 1.

AUTOMATIC DETECTION AND CLASSIFICATION OF CORONARY ARTERY PLAQUE AND STENOSIS

Since different grades of coronary artery stenosis and varying types of plaque would lead to different patient management strategies, it is therefore crucial to: (1) Detect and determine the stenosis; (2) Detailedly characterize plaques (*i.e.*, non-calcified, calcified, mixed plaques); and (3) Identify the so-called "high-risk" plaque features. Recently, there are already applications of AI techniques in related CCTA fields, including stenosis evaluation and plaque characterization. Commonly, the anatomical evaluation of coronary stenosis and quantification of plaques rely on a relative accurate segmentation and successful automatic lesion localization in CCTA images. Several vendors are developing AI-based platform for stenosis evaluation. However, the identification of "high-risk" plaques remains challenging, and only a few studies have been proposed but are of great promise with prognostic value.

Kang *et al*[5] proposed a structured learning technique for automatic detection of obstructive and non-obstructive CAD on CCTA. Taking the visual identification of lesions with stenosis ≥ 25% by three expert readers, using consensus reading, as the reference standard, the method achieved a high sensitivity (93%), specificity (95%), and diagnostic accuracy (94%), with an area under the curve (AUC) of 0.94. Zreik *et al*

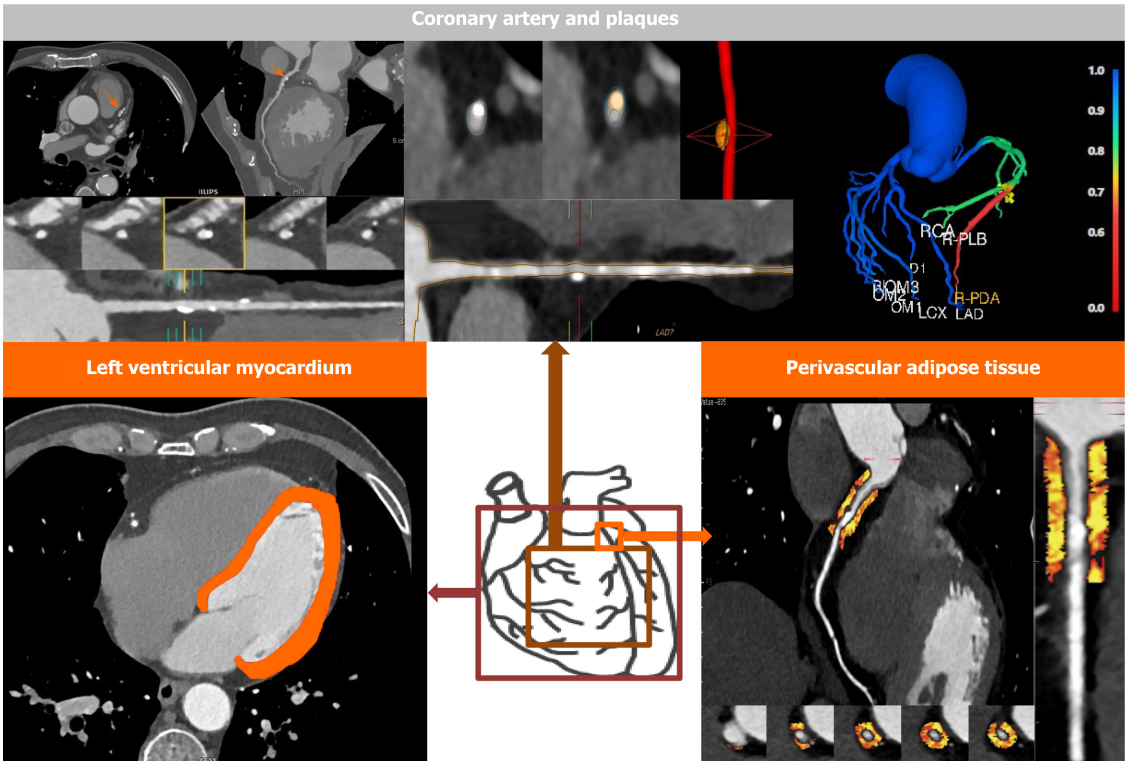

Figure 1 The application of artificial intelligence in coronary computed tomography angiography.

[6] employed a multi-task recurrent convolutional neural network to determine the stenosis severity based on the MPR view of a coronary artery extracted from the CCTA scan, as well as to automatically detect and characterize the coronary plaques. The approach achieved an accuracy of 0.80 for the determination of the anatomical significance of the coronary artery stenosis, and 0.77 for the detection and characterization of coronary plaques. Wei *et al*[7] developed a topological soft-gradient (TSG) detection method to prescreen for noncalcified plaque (NCP) candidates, which achieved AUCs of 0.87 ± 0.01 and 0.85 ± 0.01 in the training and validation sets, respectively. Jawaid *et al*[8] utilized support vector machine algorithms for automated detection of NCPs, and their approach achieved a detection accuracy of 88.4% with respect to the manual expert and a dice similarity coefficient of 83.2%.

In 2017, Kolossváry *et al*[9] investigated whether radiomics analysis improves the identification of coronary plaques with or without Napkin-ring sign (NRS). NRS is characterized as a so-called "high-risk" plaque features, which is defined as a plaque core with low CT attenuation apparently in contact with the lumen that is surrounded by a ring-shaped higher attenuation as napkin ring like in CCTA images[10,11]. However, the identification of the NRS remains challenging because it is assessed by a qualitative read of CCTA images which is affected by clinical experience and intra-/inter-reader variability[12]. Based on the segmented CCTA datasets, 8 conventional quantitative metrics and 4440 radiomic features were extracted. They found that none of the conventional quantitative parameters but 20.6% (916/4440) of radiomics features were significantly different between NRS and non-NRS plaques (Bonferroni-corrected $P < 0.0012$). In addition, almost half of the features (418/916) reached an AUC > 0.80, of which three features, including short- and long-run low gray-level emphasis and surface ratio of high attenuation voxels to total surface, exhibited excellent discriminatory value with AUCs of 0.918, 0.894, and 0.890, respectively. In 2019, the same research group validated the radiomics features extracted from CCTA in an *ex-vivo* histological study. One ML algorithm incorporating 13 parameters was superior compared with visual assessment (AUC = 0.73 *vs* 0.65) in the identification of advanced lesions[13].

DEEP LEARNING FOR AUTOMATIC CAC SCORING

CAC scoring plays a key role in risk stratification of CAD. Non-contrast-enhanced

cardiac CT, which is routinely acquired as a stand-alone test or an adjunct study prior to CCTA, is considered as the reference for quantification of CAC. CAC is defined as a high-attenuation area with > 130 HU in at least three contiguous pixels in non-contrast-enhanced cardiac CT. Recently, it has been shown that CAC can be also detected in CCTA images, which could reduce the radiation dose of a typical cardiac CT examination by 40%-50%[14]. Besides, the increased visibility of the coronary arteries in CCTA compared to non-contrast-enhanced cardiac CT could improve the identification of CAC. However, manual quantification of CAC requires substantial clinical experience to identify and make of every calcified lesion in each image slice, which is a time-consuming process. Consequently, a series of automatic methods have been proposed for CAC scoring in CCTA. Many investigations have shown promising results for clinical application in this field.

Some researchers[15,16] developed the automatic methods using two stages, including: (1) Segmentation of the coronary arteries; and (2) Identification of the CAC with the deviation from a trend line through the lumen intensity, or the voxels above a specific HU threshold, or the deviation from a model of non-calcified artery segments.

Wolterink *et al*[17,18] proposed an automatic CAC quantification method without a need for segmentation of the coronary artery tree in CCTA images using a combination of a convolutional neural network (CNN) and a Random Forest classifier. Thereafter, the same working group further extended and optimized their framework using a pair of CNNs in five ways[18], and the automatic CAC scoring in CCTA using a pair of CNNs yielded a high correlation (Pearson P = 0.950) and high consistency (intraclass correlation coefficient of 0.944) with the reference CAC scoring in non-contrast-enhanced CT.

In 2020, Fischer *et al*[19] proposed a novel fully automated algorithm using recurrent neural network with long short-term memory to detect CAC from CCTA data in a total of 565 vessels. An accuracy of 90.3% [95% confidence interval (CI): 88.0%-90.0%] was achieved on a per-vessel basis.

In summary, the CAC scoring performed on routine CCTA images without additional radiation exposure is highly desirable and the application of AI has provided considerable progress in the field and would become more influential in the clinical setting. In the near future, with the widespread application of AI techniques, CAC scoring using CCTA may eliminate the need for separate dedicated coronary calcium-scoring non-contrast enhanced CT scans.

IDENTIFICATION OF MYOCARDIAL ISCHEMIA

ML-based fractional flow reserve-CT for detection of functionally significant stenosis

It has been demonstrated that the anatomically significant appearance of a coronary stenosis is insufficient to detect hemodynamic significance and does not always equate with functional significance, which is particularly true for intermediate type coronary lesions[20,21]. Fractional flow reserve (FFR) performed during cardiac catheterization has been the reference standard in the detection of lesion-specific ischemia and is recommended for therapeutic decision-making[22]. However, the invasive measurement with a pressure wire and the relatively high cost restrict the clinical applica-tion of FFR.

Recently, novel non-invasive approaches utilizing ML algorithms for determination of FFR based on conventional CCTA images (FFR-CT) were developed and validated with a considerable diagnostic accuracy. The most popular algorithm is FFR-CT_{ML} (Figure 2). FFR-CT_{ML} was developed by Itu *et al*[23] in 2016 and provided by only one vendor (Siemens Healthineers, Germany) for research purpose. With the rapid development of AI, some FFR-CT platforms were provided for commercial use, such as the DEEPVESSE-FFR Platform provided by Keya Medical (Beijing, China). The DEEPVESSE-FFR Platform was developed by Wang *et al*[24] using MLNN + BRNN and has been commercially available since 2020.

So far, ML-based FFR-CT has been evaluated in several multi-center and single-center studies[23-35] using a threshold of ≤ 0.80 acquired from invasive FFR to detect lesion-specific ischemia. It has been demonstrated that ML-based FFR-CT performed equally in detecting flow-limiting stenosis compared with the computer fluid dynamics (CFD) based FFR-CT (FFR-CT_{CFD})[26], while the FFR-CT_{CFD} algorithm is time-consuming and heavily affected by the image quality[25,27,36]. The performance of ML-based FFR-CT in the related literature is summarized in Table 1.

Table 1 Summary of the current literature on machine learning-based fractional flow reserve-computed tomography

Ref.	Journal	Prospective	Multi- or single center	Platform	No. of patients	No. of vessels	Compared with CT-FFR_{CFD}	Accuracy	AUC
Itu *et al*[23], 2016	*Journal Application Physiology*	No	Single center	-	87	125	Yes	Per-lesion: 83%	Per-lesion: 0.90
Coenen *et al* [25], 2018	*Circulation: Cardiovascular Imaging*	Yes	The MACHINE registry	cFFR, version 2.1, Siemens	351	525	Yes	Per-lesion: 78%Per-patient: 85%	Per-lesion: 0.84
Tesche *et al* [26], 2018	*Radiology*	No	Single Center	cFFR, version 1.4, Siemens	85	104	Yes	Per-lesion: 88%; Per-patient: 92%	Per-lesion: 0.89; Per-patient: 0.91
Mastrodicasa *et al*[34], 2019	*Journal of Cardiovascular Computed Tomograph*	No	Single center	cFFR, version 3.0, Siemens	10/40	160	No	IRIS: 82%; FBP: 82%	-
Baumann *et al* [32], 2019	*European Journal of Radiology*	No	The MACHINE registry	cFFR, version 2.1, Siemens	351	525	No	-	Per-patient: Women:0.83; Men: 0.83
Doeberitz *et al* [27], 2019	*European Radiology*	No	Single center	cFFR, version 2.1, Siemens	48	103	No	-	Per-lesion: 0.93
Wang *et al* [24], 2019	*Journal of Geriatric Cardiology*	Yes	Single center	DEEPVESSE-FFR Platform	63	71	No	Per-lesion: 89%; Per-patient: 87%	Per-lesion: 0.93; Per-patient: 0.93
Tesche *et al* [30], 2020	*Journals of the American College of Cardiology: Cardiovascular Imaging*	Yes	The MACHINE registry	cFFR, version 2.1, Siemens	314	482	No	Per-lesion: 78%; CAC ≥ 400: 76%CAC 0-100: 79%; CAC 100-400: 76%	Total: 0.84 CAC ≥ 400: 0.71; CAC 0-400: 0.85
De Geer *et al* [31], 2019	*American Journal of Roentgenology*	No	The MACHINE registry	cFFR, version 2.1, Siemens	351	525	No	Total: 78%; 80 kv: 86%; 100 kv: 77%; 120 kv: 78%	Total: 0.84; 80 kv: 0.90; 100 kv: 0.82; 120 kv: 0.84
Xu *et al*[33], 2020	*European Radiology*	No	10 individual centers across China	cFFR, version 3.2.0, Siemens	437	570	No	Total: 89%; High quality: 94%; Low quality: 83%	Total: 0.89; High quality: 0.93; Low quality: 0.80
Kumamaru *et al*[28], 2020	*European Heart Journal - Cardiovascular Imaging*	No	Multi-center	Python 3.6	131	-	No	Per-patient: 76%	Per-patient: 0.78
Li *et al*[29], 2021	*Acta Radiologica*	No	Single center	DEEPVESSE-FFR Platform	73	85	No	Per-lesion: 92%; Per-patient: 91%	Per-lesion: 0.96
Xu *et al*[35], 2020	*European Radiology*	No	A Chinese multicenter study	cFFR, version 3.1.0, Siemens	442	544	No	Per lesion: 90%	-

IRIS: Iterative reconstruction in image space; FBP: Filtered back projection; CAC: Coronary artery calcium; FFR: Fractional flow reserve; AUC: Area under the curve; CT: Computed tomography.

In addition, the influences of CT reconstruction algorithms, image quality, tube voltage, coronary calcium, and gender on the diagnostic performance of FFR-CT_{ML} were investigated in several studies. In a sub-study of MACHINE Registry, Tesche *et al* [30] examined the impact of calcification on CT-FFR_{ML} determination and concluded that CT-FFR_{ML} revealed a statistically significant different (P = 0.04) performance as Agatston calcium score increased: The AUC in high Agatston scores (CAC ≥ 400) was 0.71 (95%CI: 0.57-0.85) and in low-to-intermediate Agatston scores (CAC > 0 to < 400) was 0.85 (95%CI: 0.82-0.89). In another sub-study of MACHINE Registry, De Geer *et al* [31] examined the impact of different tube voltages on CT-FFRML determination and concluded that performance does not vary significantly between tube voltages of 100 kVp (AUC: 0.82) and 120 kVp (AUC: 0.84), while the AUC was 0.90 in examination with a tube voltage of 80 kVp. Based on data of the MACHINE Registry, Baumann *et al*

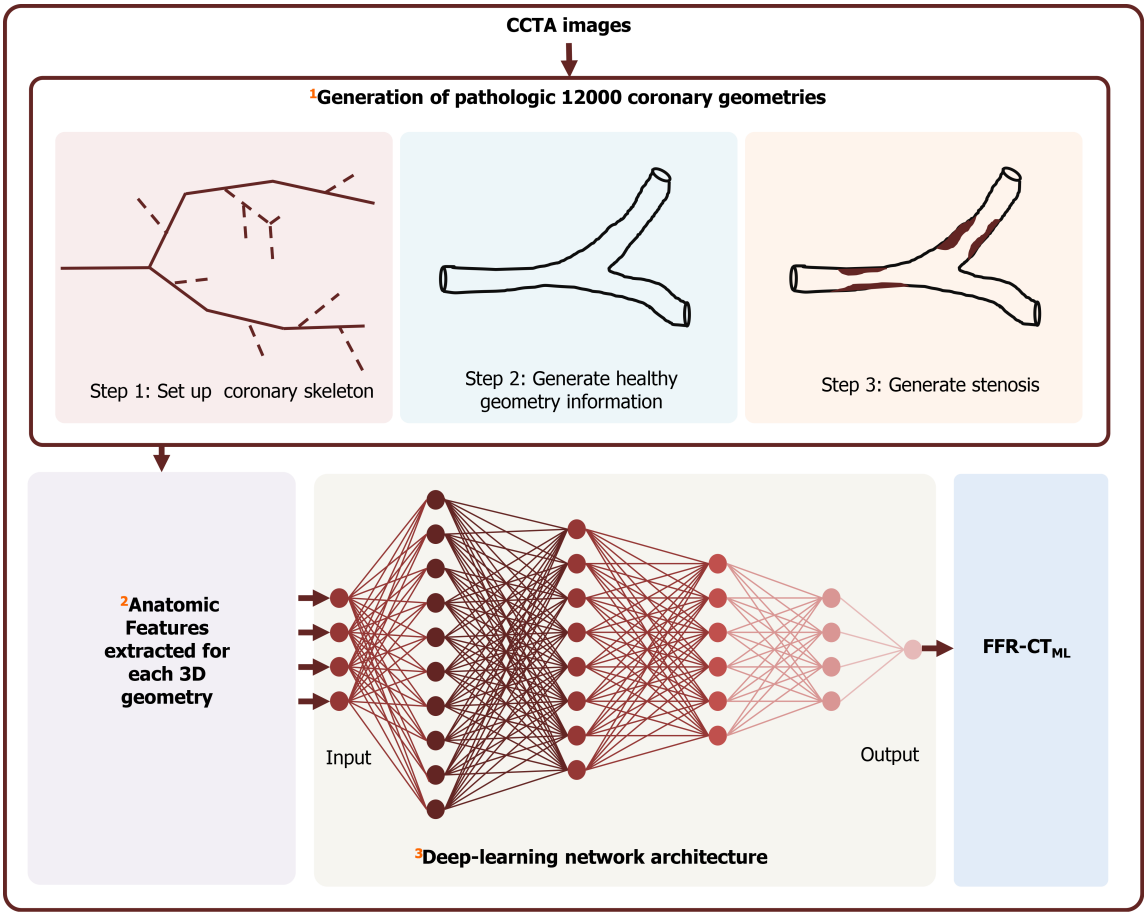

Figure 2 The workflow of the fractional flow reserve-computed tomography derivation. [1]A total of 12000 coronary anatomies were generated; [2]twenty-eight geometric features were extracted from the synthetically generated database; [3]a deep neural network with four hidden layers was used to train the machine learning-based model. FFR-CT: Fractional flow reserve-computed tomography; CCTA: Coronary computed tomography angiography.

[32] evaluated the impact of gender on the performance of FFRCTML and they found that FFRCTML performs equally in men and women (both with an AUC of 0.83). In a retrospective Chinese multicenter study, Xu *et al*[33] investigated the effect of image quality on the diagnostic performance of FFRCTML in 437 patients with 570 vessels. They found that the AUC of high-quality images [0.93 (95%CI: 0.88-0.98), n = 159] was significantly (P = 0.02) superior to that of low-quality images [0.80 (95%CI: 0.70-0.90), n = 92]. And CCTA with a score ≥ 3, intracoronary enhancement degree of 300–400 HU, and heart rate below 70 bpm at scanning could be of great benefit to more accurate FFRCTML analysis. In a retrospective single center study, Mastrodicasa *et al*[34] evaluated the influence of different CT reconstruction algorithms on the performance of CT-FFR$_{ML}$ in 40 CCTA datasets. CT-FFRML values were significantly different between iterative reconstruction in image space (IRIS) and filtered back projection algorithms, whereas no difference was observed in diagnostic accuracy (both 81.8%, P = 1.000). Additionally, they found that IRIS improved CT-FFRML post-processing speed significantly.

It should be mentioned that CT-FFR$_{ML}$ value for each location along the coronary is trained when taking the CT-FFR$_{CFD}$ as ground truth. Although the diagnostic accuracy of CT-FFR derived using deep learning (DL) methods was validated in several studies, it is still susceptible to the CCTA scanning factors. In the future, more attention should be paid to the widespread use of a local software solution that allows for image-variation and user-variation.

OTHER AI ALGORITHMS FOR PREDICTION OF MYOCARDIAL ISCHEMIA

Except for the ML based FFR-CT platforms described above, some other AI algorithms were developed recently for prediction of myocardial ischemia. These approaches are in early stage but show better interpretability, which were established *via* an

integration of qualitative or quantitative features derived from CCTA images and clinical factors.

In 2018, Dey *et al*[37] developed an integrated ML ischemia risk score (ML-IRS) from quantitative plaque measures using a supervised learning process to predict functionally significant stenosis in a prospective multicenter trial of 254 patients with 484 vessels. The ML-IRS exhibited a higher AUC (0.84) than conventional CCTA measures, including stenosis (0.76), LD-NCP volume (0.77), total plaque volume (0.74), and pre-test likelihood of CAD (0.63), for predicting lesion-specific ischemia by invasive FFR. Thereafter, the ML-IRS was integrated into coronary plaque analysis research software for generating a percent probability of pathological FFR on CCTA data.

In 2019, van Hamersvelt *et al*[38] proposed a DL method based on the LVM in resting CCTA images to identify functionally significant coronary artery stenosis using 126 patients. The DL approach achieved a higher AUC of 0.76 compared to degree of stenosis (AUC = 0.68).

In 2020, Shu *et al*[39] established a radiomics nomogram based on myocardial segments for predicting chronic myocardial ischemia using multivariate logistic regression. The accuracy of the nomogram for distinguishing chronic myocardial ischemia from normal myocardium was 0.839, 0.832, and 0.816 in the training, test, and validation cohorts, respectively.

PROGNOSTIC SIGNIFICANCE

PVAT-based radiomics for improving cardiac risk prediction

Early detection of vascular inflammation, which is a major contributor to atherogenesis and atherosclerotic plaque rupture[40,41], would enable better cardiovascular risk stratification[42]. The vascular inflammation can be detected by characterizing the phenotypic changes in PVAT using the fat attenuation index (FAI) in routine CCTA images[43,44]. FAI was defined as the average attenuation of all voxels with attenuation values between -190 HU and -30 HU located within a radial distance from the outer coronary artery wall equal to the average diameter of the respective vessel, as described previously[43,44]. However, FAI is an average of the voxel intensity values and does not account for the complex spatial relationship among voxels.

Recently, some studies investigated whether radiomics analysis could help to extract more information from the PVAT that cannot be captured by human eyes. The radiomics features surrounding PVAT mainly include two parts: (1) PVAT surrounding the standardized coronary segments, which was often investigated at a per-patient level; and (2) PVAT around the target lesion, which was at a per-lesion level.

As for the per-patient level, Oikonomou *et al*[45] developed an AI-powered radiotranscriptomic signature for predicting cardiac risk based on the radiomics features extracted from PVAT around the proximal to distal right coronary artery (RCA) and the left coronary artery in CCTA images. A fat radiomic profile (FRP) was established, using random forest model based on the features extracted from the standardized coronary segments, to distinguish the 101 patients who experienced major adverse cardiac events (MACE) within 5 years from 101 matched controls. The FRP was significantly associated with the risk of MACE [adjusted hazard ratio (HR): 1.12, 95%CI: 1.08-1.15, $P < 0.001$]. And patients with an FRP ≥ 0.63 had a 10.8-fold higher risk of MACE than those with an FRP < 0.63, after adjusted for clinical factors. The AUC of FRP in predicting MACE was 0.774 (95%CI: 0.622-0.926) in the external validation dataset (20% of the 202 samples). When added to the traditional model, FRP improved the distinguishing performance from an AUC of 0.754 to 0.880. Additionally, they found that FRP was significantly higher in 44 patients with acute MI compared with 44 controls ($P < 0.001$), but unlike FAI, FRP remained unchanged 6 mo later in 16 patients with acute MI (AMI), confirming that FRP detects persistent PVAT changes that cannot be captured by FAI.

As for the per-lesion level, in 2020, Lin *et al*[46] further explored the prognostic value of the radiomics features of PVAT around not only the standardized coronary segments but also lesions in a prospective case-control study. They found no significant difference between the PVAT radiomics features of culprit and non-culprit lesions in patients with AMI, lending further support to the pan-coronary inflammatory hypothesis. But on the other hand, as for the per-patient level, patients with AMI (n = 60) have a distinct PVAT radiomics phenotype surrounding the proximal RCA compared with patients with stable (matched, n = 60) or no CAD (matched, n =

60). Among the three models that they developed, the PVAT-based radiomics model (AUC: 0.87) outperforms the clinical model (AUC: 0.76) and the combined model incorporating clinical factors and PVAT attenuation (AUC: 0.77) in identifying AMI with stable CAD and controls. Additionally, after a 6-mo follow-up of patients with AMI, no significant change was observed in the radiomics features of PVAT surrounding the proximal RCA or non-culprit lesions.

QUANTITATIVE CT FEATURES-BASED ML FOR OUTCOME PREDICTION

Information extracted from CCTA images along with other clinical factors are associated with prognosis, and AI technology demonstrated great potential to enhance decision-making and improve patient outcomes. Currently, the prognostic value of ML algorithms using quantitative CCTA features together with clinical variables was investigated by researchers in several studies[47-53], in which promising results were obtained. The ML algorithms performed better than traditional predictors, not only for short-term treatment decisions but also for long-term risk predictions, as summarized in Table 2.

One of the first major studies using CCTA based ML approach for prognosis evaluation is a large prospective multi-center study conducted by Motwani *et al*[48] in 2017. They developed an ML model in CCTA to predict 5-year all-cause mortality using a dataset of 10030 patients with suspected CAD from the CONFIRM registry (Coronary CT Angiography Evaluation for Clinical Outcomes: An International Multicenter). The ML model was established after an automated feature selection procedure based on 44 CCTA-derived parameters and 25 clinical parameters. One summary score for clinical parameters (Framingham risk score, FRS) and three composite CCTA-based scores [including the segment stenosis score (SSS), the segment involvement score (SIS), and the modified Duke prognostic CAD index (DI)] were derived. The ML model exhibited a significant higher AUC compared with the conventional scores alone for predicting 5-year all-cause mortality (ML: 0.79 *vs* FRS: 0.61, SSS: 0.64, SIS: 0.64, and DI: 0.62; $P < 0.001$).

Two years later, in 2019, Johnson *et al*[49] developed another ML model using 64 vessel features derived from CCTA images, to discriminate between patients with and without subsequent death or cardiovascular events in a retrospective single-center study with 6892 patients. The performance of the ML model was compared with that of Coronary Artery Disease Reporting and Data System (CAD-RADS) score. For prediction of all-cause mortality, the AUC of the ML model was significantly higher than that of CAD-RADS (0.77 *vs* 0.72, $P < 0.001$). For prediction of coronary artery deaths, the AUC was significantly higher for the ML model than for CAD-RADS (0.85 *vs* 0.79, $P < 0.001$).

In 2020, Commandeur *et al*[52] developed an ML model integrating clinical parameters with quantitative imaging-based variables for predicting events of long-term risk of MI and cardiac death in asymptomatic subjects using the dataset with 1912 cases from the randomized EISNER trial. The ML model obtained a significantly higher AUC than atherosclerotic cardiovascular disease (ASCVD) risk and CAC score for predicting events (ML: 0.82; ASCVD: 0.77; CAC: 0.77; $P < 0.05$). Subjects with a higher ML score had a significant high hazard of suffering events (HR: 10.38, $P < 0.001$).

As for the short-term decision-making, in 2020, Kwan *et al*[53] examined whether the ML-IRS, developed by Dey *et al*[37] in 2018, as described previously (Figures 1 and 2), can predict revascularization in patients referred to ICA after CCTA in a prospective dual-center study of 352 patients with 1056 analyzable vessels. It would be beneficial to effectively identify the patients who were referred for standard clinical CCTA followed by ICA due to decision by a primary treating physician but did not receive revascularization, because those patients are a high-cost population with low yield from the invasive procedure. The results indicated that ML-IRS, when added to the traditional risk model, significantly improve the prediction of future revascularization with an increased AUC from 0.69 (95%CI: 0.65-0.72) to 0.78 (95%CI: 0.75-0.81) ($P < 0.0001$).

Overall, the application of AI in CCTA has a potential future for improving the short-term risk stratification and long-term prognostic evaluation. The ML algorithms that have been proposed should be validated and tested in real world with larger external cohorts including diversity of patients so as to make sure the models be optimized and generalized.

Table 2 summary of the current literature on the prognostic value of machine learning algorithms in coronary computed tomography angiography

Ref.	Journal	Prospective	Multi Center	No. of Patients	No. of Events	Algorithm	Endpoint	Follow-up time	Performance
Motwani *et al* [48], 2017	*European Heart Journal*	Yes	Yes	10030	745 died	LogitBoost	5-yr all-cause mortality	5.4 ± 1.4 yr	AUC = 0.79
van Rosendael *et al*[47], 2018	*Journal of Cardiovascular Computed Tomograph*	Yes	Yes	8844	350 death and 259 non-fatal MI	XGBoost	MI and death	4.6 ± 1.5 yr	AUC = 0.77
Johnson *et al* [49], 2019	*Radiology*	No	No	6892	380 died of all causes and 70 died of CAD	Logistic regression, KNN, Bagged trees, and classification neural network	Death or cardiovascular events	9.0 yr (interquartile range, 8.2–9.8 yr)	For all-cause mortality: AUC = 0.77; For CAD deaths: AUC = 0.85
van Assen *et al* [50], 2019	*European Journal of Radiology*	No	No	45	16 MACEs	Regression analysis	MACE	12 mo	AUC = 0.94
von Knebel Doeberitz *et al* [51], 2019	*The American Journal of Cardiology*	No	No	82	18 MACEs	Integration of CT-FFR, stenosis ≥ 50% and plaque markers	MACE	18.5 mo (interquartile range 11.5 to 26.6 mo)	AUC = 0.94
Commandeur *et al*[52], 2020	*Cardiovascular Research*	Yes		1912	76 MI and/or cardiac death	ML	Long-term risk of MI and cardiac death	14.5 ± 2 yr	AUC = 0.82
Kwan *et al* [53], 2021	*European Radiology*	Yes	Yes	352		ML	Future revascularization		AUC = 0.78

XGBoost: Extreme gradient boosting; KNN: K-nearest neighbors; ML: Machine learning; AUC: Area under the curve; MACE: Major adverse cardiac events; CT-FFR: Computed tomography-fractional flow reserve; CAD: Coronary artery disease; MI: Myocardial infarction.

CONCLUSION

Current AI applications in CCTA images are mostly designed in two dimensions: (1) For the radiologists, AI is applied to improve efficiency and reduce workload *via* optimizing the clinical workflow, such as improvement of image reconstruction from lower quality to high quality (*e.g.*, low-dose acquisition or motion artifacts) and structured reporting; and (2) For the patients, AI is utilized to increase benefit and improve prognostic evaluation *via* providing valuable diagnostic information more accurately, such as detection of anatomic and functional stenosis, quantification of plaques, and estimation of the vascular inflammation.

In this review, we mainly focused on the second dimension which is patient oriented. AI algorithms in CCTA images provide information in a more objective, reproducible, and rational manner compared to human perception, and exhibits its potential to outperform human in several cardiac fields. However, CCTA imaging lagged behind cancer imaging in the clinical translational of AI-based methods, especially the radiomics analysis. It has long been demonstrated in the field of cancer imaging that radiomics signatures are superior to traditional factors in predicting outcomes of patients. But only a few studies using radiomics analysis have been conducted in CCTA images. Considering that regions of interest (ROIs) segmented before the extraction of radiomics features, can be drawn along the edge of the tumor in cancer imaging generally, in CCTA images the selection of ROIs brings about challenges. Researchers hereby performed radiomics analysis around the PVAT or LVM or plaques. And recently, several groups succeeded in developing automated segmentation of PVAT and LVM, which provides probabilities to explore more novel non-invasive predictors for improvement of risk stratification and prognosis in patients with CAD.

Additionally, FFR-CT driven by AI is a hot topic in recent years. Various FFR-CT platforms are developed and adding into the clinical diagnostic workflow for not only research purpose but also commercial use. In the near future, the FFR-CT platforms

would bring major changes in the way to make decisions for patients with CAD before invasive coronary angiography.

However, before AI solutions can be truly widely implemented in daily clinical workflow or the reading room, several issues should be noted: (1) The algorithms need to be carefully validated in multi-center studies or large clinical trials to ensure the robustness and generalization; (2) The approval of clinical application is required to prove the accuracy and safety of the AI products; and (3) The legal and ethical issues should be taken into consideration.

In summary, AI offers the possibility to optimize clinical workflow and provide precise information for diagnostic and treatment, which will benefit both radiologists and patients. However, it is pertinent to note that AI will not simply substitute the cardiac radiologists, and human support or supervision is still needed. Rather, the cardiac radiologists need to be fully aware of the strengths and limitations of AI.

ACKNOWLEDGEMENTS

First, I want to show my great gratitude to my teacher Dr. Hou, a responsible and respectable scholar, offering valuable suggestions for revision. In addition, I am grateful to Guo Y for her contribution to the writing process. Also, I wish to thank those who have offered me great help and support, such as editors, reviewers, and publishers.

REFERENCES

1 **Padley SPG**, Roditi G, Nicol ED; BSCI/BSCCT. Chest pain of recent onset: assessment and diagnosis (CG95). A step change in the requirement for cardiovascular CT. *Clin Radiol* 2017; **72**: 751-753 [PMID: 28647044 DOI: 10.1016/j.crad.2017.04.020]

2 **Knuuti J**, Wijns W, Saraste A, Capodanno D, Barbato E, Funck-Brentano C, Prescott E, Storey RF, Deaton C, Cuisset T, Agewall S, Dickstein K, Edvardsen T, Escaned J, Gersh BJ, Svitil P, Gilard M, Hasdai D, Hatala R, Mahfoud F, Masip J, Muneretto C, Valgimigli M, Achenbach S, Bax JJ; ESC Scientific Document Group. 2019 ESC Guidelines for the diagnosis and management of chronic coronary syndromes. *Eur Heart J* 2020; **41**: 407-477 [PMID: 31504439 DOI: 10.1093/eurheartj/ehz425]

3 **Lamata P**. Teaching cardiovascular medicine to machines. *Cardiovasc Res* 2018; **114**: e62-e64 [PMID: 29850780 DOI: 10.1093/cvr/cvy127]

4 **Deo RC**. Machine Learning in Medicine. *Circulation* 2015; **132**: 1920-1930 [PMID: 26572668 DOI: 10.1161/CIRCULATIONAHA.115.001593]

5 **Kang D**, Dey D, Slomka PJ, Arsanjani R, Nakazato R, Ko H, Berman DS, Li D, Kuo CC. Structured learning algorithm for detection of nonobstructive and obstructive coronary plaque lesions from computed tomography angiography. *J Med Imaging (Bellingham)* 2015; **2**: 014003 [PMID: 26158081 DOI: 10.1117/1.JMI.2.1.014003]

6 **Zreik M**, van Hamersvelt RW, Wolterink JM, Leiner T, Viergever MA, Isgum I. A Recurrent CNN for Automatic Detection and Classification of Coronary Artery Plaque and Stenosis in Coronary CT Angiography. *IEEE Trans Med Imaging* 2019; **38**: 1588-1598 [PMID: 30507498 DOI: 10.1109/TMI.2018.2883807]

7 **Wei J**, Zhou C, Chan HP, Chughtai A, Agarwal P, Kuriakose J, Hadjiiski L, Patel S, Kazerooni E. Computerized detection of noncalcified plaques in coronary CT angiography: evaluation of topological soft gradient prescreening method and luminal analysis. *Med Phys* 2014; **41**: 081901 [PMID: 25086532 DOI: 10.1118/1.4885958]

8 **Jawaid MM**, Riaz A, Rajani R, Reyes-Aldasoro CC, Slabaugh G. Framework for detection and localization of coronary non-calcified plaques in cardiac CTA using mean radial profiles. *Comput Biol Med* 2017; **89**: 84-95 [PMID: 28797740 DOI: 10.1016/j.compbiomed.2017.07.021]

9 **Kolossváry M**, Karády J, Szilveszter B, Kitslaar P, Hoffmann U, Merkely B, Maurovich-Horvat P. Radiomic Features Are Superior to Conventional Quantitative Computed Tomographic Metrics to Identify Coronary Plaques With Napkin-Ring Sign. *Circ Cardiovasc Imaging* 2017; **10**: e006843 [PMID: 29233836 DOI: 10.1161/CIRCIMAGING.117.006843]

10 **Narula J**, Achenbach S. Napkin-ring necrotic cores: defining circumferential extent of necrotic cores in unstable plaques. *JACC Cardiovasc Imaging* 2009; **2**: 1436-1438 [PMID: 20083080 DOI: 10.1016/j.jcmg.2009.10.004]

11 **Maurovich-Horvat P**, Hoffmann U, Vorpahl M, Nakano M, Virmani R, Alkadhi H. The napkin-ring sign: CT signature of high-risk coronary plaques? *JACC Cardiovasc Imaging* 2010; **3**: 440-444 [PMID: 20394906 DOI: 10.1016/j.jcmg.2010.02.003]

12 **Puchner SB**, Liu T, Mayrhofer T, Truong QA, Lee H, Fleg JL, Nagurney JT, Udelson JE, Hoffmann U, Ferencik M. High-risk plaque detected on coronary CT angiography predicts acute coronary syndromes independent of significant stenosis in acute chest pain: results from the ROMICAT-II trial.

J Am Coll Cardiol 2014; **64**: 684-692 [PMID: 25125300 DOI: 10.1016/j.jacc.2014.05.039]

13 **Kolossváry M**, Karády J, Kikuchi Y, Ivanov A, Schlett CL, Lu MT, Foldyna B, Merkely B, Aerts HJ, Hoffmann U, Maurovich-Horvat P. Radiomics versus Visual and Histogram-based Assessment to Identify Atheromatous Lesions at Coronary CT Angiography: An ex Vivo Study. *Radiology* 2019; **293**: 89-96 [PMID: 31385755 DOI: 10.1148/radiol.2019190407]

14 **Voros S**, Qian Z. Agatston score tried and true: by contrast, can we quantify calcium on CTA? *J Cardiovasc Comput Tomogr* 2012; **6**: 45-47 [PMID: 22264631 DOI: 10.1016/j.jcct.2011.12.002]

15 **Ahmed W**, de Graaf MA, Broersen A, Kitslaar PH, Oost E, Dijkstra J, Bax JJ, Reiber JH, Scholte AJ. Automatic detection and quantification of the Agatston coronary artery calcium score on contrast computed tomography angiography. *Int J Cardiovasc Imaging* 2015; **31**: 151-161 [PMID: 25159031 DOI: 10.1007/s10554-014-0519-4]

16 **Eilot D**, Goldenberg R. Fully automatic model-based calcium segmentation and scoring in coronary CT angiography. *Int J Comput Assist Radiol Surg* 2014; **9**: 595-608 [PMID: 24203575 DOI: 10.1007/s11548-013-0955-y]

17 **Wolterink JM**, Leiner T, de Vos BD, Coatrieux JL, Kelm BM, Kondo S, Salgado RA, Shahzad R, Shu H, Snoeren M, Takx RA, van Vliet LJ, van Walsum T, Willems TP, Yang G, Zheng Y, Viergever MA, Išgum I. An evaluation of automatic coronary artery calcium scoring methods with cardiac CT using the orCaScore framework. *Med Phys* 2016; **43**: 2361 [PMID: 27147348 DOI: 10.1118/1.4945696]

18 **Wolterink JM**, Leiner T, de Vos BD, van Hamersvelt RW, Viergever MA, Išgum I. Automatic coronary artery calcium scoring in cardiac CT angiography using paired convolutional neural networks. *Med Image Anal* 2016; **34**: 123-136 [PMID: 27138584 DOI: 10.1016/j.media.2016.04.004]

19 **Fischer AM**, Eid M, De Cecco CN, Gulsun MA, van Assen M, Nance JW, Sahbaee P, De Santis D, Bauer MJ, Jacobs BE, Varga-Szemes A, Kabakus IM, Sharma P, Jackson LJ, Schoepf UJ. Accuracy of an Artificial Intelligence Deep Learning Algorithm Implementing a Recurrent Neural Network With Long Short-term Memory for the Automated Detection of Calcified Plaques From Coronary Computed Tomography Angiography. *J Thorac Imaging* 2020; **35** Suppl 1: S49-S57 [PMID: 32168163 DOI: 10.1097/RTI.0000000000000491]

20 **Meijboom WB**, Van Mieghem CA, van Pelt N, Weustink A, Pugliese F, Mollet NR, Boersma E, Regar E, van Geuns RJ, de Jaegere PJ, Serruys PW, Krestin GP, de Feyter PJ. Comprehensive assessment of coronary artery stenoses: computed tomography coronary angiography versus conventional coronary angiography and correlation with fractional flow reserve in patients with stable angina. *J Am Coll Cardiol* 2008; **52**: 636-643 [PMID: 18702967 DOI: 10.1016/j.jacc.2008.05.024]

21 **Conte E**, Sonck J, Mushtaq S, Collet C, Mizukami T, Barbato E, Tanzilli A, Nicoli F, De Bruyne B, Andreini D. FFR_{CT} and CT perfusion: A review on the evaluation of functional impact of coronary artery stenosis by cardiac CT. *Int J Cardiol* 2020; **300**: 289-296 [PMID: 31466886 DOI: 10.1016/j.ijcard.2019.08.018]

22 **Tonino PA**, De Bruyne B, Pijls NH, Siebert U, Ikeno F, van' t Veer M, Klauss V, Manoharan G, Engstrøm T, Oldroyd KG, Ver Lee PN, MacCarthy PA, Fearon WF; FAME Study Investigators. Fractional flow reserve versus angiography for guiding percutaneous coronary intervention. *N Engl J Med* 2009; **360**: 213-224 [PMID: 19144937 DOI: 10.1056/NEJMoa0807611]

23 **Itu L**, Rapaka S, Passerini T, Georgescu B, Schwemmer C, Schoebinger M, Flohr T, Sharma P, Comaniciu D. A machine-learning approach for computation of fractional flow reserve from coronary computed tomography. *J Appl Physiol (1985)* 2016; **121**: 42-52 [PMID: 27079692 DOI: 10.1152/japplphysiol.00752.2015]

24 **Wang ZQ**, Zhou YJ, Zhao YX, Shi DM, Liu YY, Liu W, Liu XL, Li YP. Diagnostic accuracy of a deep learning approach to calculate FFR from coronary CT angiography. *J Geriatr Cardiol* 2019; **16**: 42-48 [PMID: 30800150 DOI: 10.11909/j.issn.1671-5411.2019.01.010]

25 **Coenen A**, Kim YH, Kruk M, Tesche C, De Geer J, Kurata A, Lubbers ML, Daemen J, Itu L, Rapaka S, Sharma P, Schwemmer C, Persson A, Schoepf UJ, Kepka C, Hyun Yang D, Nieman K. Diagnostic Accuracy of a Machine-Learning Approach to Coronary Computed Tomographic Angiography-Based Fractional Flow Reserve: Result From the MACHINE Consortium. *Circ Cardiovasc Imaging* 2018; **11**: e007217 [PMID: 29914866 DOI: 10.1161/CIRCIMAGING.117.007217]

26 **Tesche C**, De Cecco CN, Baumann S, Renker M, McLaurin TW, Duguay TM, Bayer RR 2nd, Steinberg DH, Grant KL, Canstein C, Schwemmer C, Schoebinger M, Itu LM, Rapaka S, Sharma P, Schoepf UJ. Coronary CT Angiography-derived Fractional Flow Reserve: Machine Learning Algorithm versus Computational Fluid Dynamics Modeling. *Radiology* 2018; **288**: 64-72 [PMID: 29634438 DOI: 10.1148/radiol.2018171291]

27 **von Knebel Doeberitz PL**, De Cecco CN, Schoepf UJ, Duguay TM, Albrecht MH, van Assen M, Bauer MJ, Savage RH, Pannell JT, De Santis D, Johnson AA, Varga-Szemes A, Bayer RR, Schönberg SO, Nance JW, Tesche C. Coronary CT angiography-derived plaque quantification with artificial intelligence CT fractional flow reserve for the identification of lesion-specific ischemia. *Eur Radiol* 2019; **29**: 2378-2387 [PMID: 30523456 DOI: 10.1007/s00330-018-5834-z]

28 **Kumamaru KK**, Fujimoto S, Otsuka Y, Kawasaki T, Kawaguchi Y, Kato E, Takamura K, Aoshima C, Kamo Y, Kogure Y, Inage H, Daida H, Aoki S. Diagnostic accuracy of 3D deep-learning-based fully automated estimation of patient-level minimum fractional flow reserve from coronary computed tomography angiography. *Eur Heart J Cardiovasc Imaging* 2020; **21**: 437-445 [PMID: 31230076 DOI: 10.1093/ehjci/jez160]

29 **Li Y**, Qiu H, Hou Z, Zheng J, Li J, Yin Y, Gao R. Additional value of deep learning computed

tomographic angiography-based fractional flow reserve in detecting coronary stenosis and predicting outcomes. *Acta Radiol* 2021; 284185120983977 [PMID: 33423530 DOI: 10.1177/0284185120983977]

30 **Tesche C**, Otani K, De Cecco CN, Coenen A, De Geer J, Kruk M, Kim YH, Albrecht MH, Baumann S, Renker M, Bayer RR, Duguay TM, Litwin SE, Varga-Szemes A, Steinberg DH, Yang DH, Kepka C, Persson A, Nieman K, Schoepf UJ. Influence of Coronary Calcium on Diagnostic Performance of Machine Learning CT-FFR: Results From MACHINE Registry. *JACC Cardiovasc Imaging* 2020; **13**: 760-770 [PMID: 31422141 DOI: 10.1016/j.jcmg.2019.06.027]

31 **De Geer J**, Coenen A, Kim YH, Kruk M, Tesche C, Schoepf UJ, Kepka C, Yang DH, Nieman K, Persson A. Effect of Tube Voltage on Diagnostic Performance of Fractional Flow Reserve Derived From Coronary CT Angiography With Machine Learning: Results From the MACHINE Registry. *AJR Am J Roentgenol* 2019; **213**: 325-331 [PMID: 31039021 DOI: 10.2214/AJR.18.20774]

32 **Baumann S**, Renker M, Schoepf UJ, De Cecco CN, Coenen A, De Geer J, Kruk M, Kim YH, Albrecht MH, Duguay TM, Jacobs BE, Bayer RR, Litwin SE, Weiss C, Akin I, Borggrefe M, Yang DH, Kepka C, Persson A, Nieman K, Tesche C. Gender differences in the diagnostic performance of machine learning coronary CT angiography-derived fractional flow reserve -results from the MACHINE registry. *Eur J Radiol* 2019; **119**: 108657 [PMID: 31521876 DOI: 10.1016/j.ejrad.2019.108657]

33 **Xu PP**, Li JH, Zhou F, Jiang MD, Zhou CS, Lu MJ, Tang CX, Zhang XL, Yang L, Zhang YX, Wang YN, Zhang JY, Yu MM, Hou Y, Zheng MW, Zhang B, Zhang DM, Yi Y, Xu L, Hu XH, Liu H, Lu GM, Ni QQ, Zhang LJ. The influence of image quality on diagnostic performance of a machine learning-based fractional flow reserve derived from coronary CT angiography. *Eur Radiol* 2020; **30**: 2525-2534 [PMID: 32006167 DOI: 10.1007/s00330-019-06571-4]

34 **Mastrodicasa D**, Albrecht MH, Schoepf UJ, Varga-Szemes A, Jacobs BE, Gassenmaier S, De Santis D, Eid MH, van Assen M, Tesche C, Mantini C, De Cecco CN. Artificial intelligence machine learning-based coronary CT fractional flow reserve (CT-FFR_{ML}): Impact of iterative and filtered back projection reconstruction techniques. *J Cardiovasc Comput Tomogr* 2019; **13**: 331-335 [PMID: 30391256 DOI: 10.1016/j.jcct.2018.10.026]

35 **Di Jiang M**, Zhang XL, Liu H, Tang CX, Li JH, Wang YN, Xu PP, Zhou CS, Zhou F, Lu MJ, Zhang JY, Yu MM, Hou Y, Zheng MW, Zhang B, Zhang DM, Yi Y, Xu L, Hu XH, Yang J, Lu GM, Ni QQ, Zhang LJ. The effect of coronary calcification on diagnostic performance of machine learning-based CT-FFR: a Chinese multicenter study. *Eur Radiol* 2021; **31**: 1482-1493 [PMID: 32929641 DOI: 10.1007/s00330-020-07261-2]

36 **Gaur S**, Øvrehus KA, Dey D, Leipsic J, Bøtker HE, Jensen JM, Narula J, Ahmadi A, Achenbach S, Ko BS, Christiansen EH, Kaltoft AK, Berman DS, Bezerra H, Lassen JF, Nørgaard BL. Coronary plaque quantification and fractional flow reserve by coronary computed tomography angiography identify ischaemia-causing lesions. *Eur Heart J* 2016; **37**: 1220-1227 [PMID: 26763790 DOI: 10.1093/eurheartj/ehv690]

37 **Dey D**, Gaur S, Ovrehus KA, Slomka PJ, Betancur J, Goeller M, Hell MM, Gransar H, Berman DS, Achenbach S, Botker HE, Jensen JM, Lassen JF, Norgaard BL. Integrated prediction of lesion-specific ischaemia from quantitative coronary CT angiography using machine learning: a multicentre study. *Eur Radiol* 2018; **28**: 2655-2664 [PMID: 29352380 DOI: 10.1007/s00330-017-5223-z]

38 **van Hamersvelt RW**, Zreik M, Voskuil M, Viergever MA, Išgum I, Leiner T. Deep learning analysis of left ventricular myocardium in CT angiographic intermediate-degree coronary stenosis improves the diagnostic accuracy for identification of functionally significant stenosis. *Eur Radiol* 2019; **29**: 2350-2359 [PMID: 30421020 DOI: 10.1007/s00330-018-5822-3]

39 **Shu ZY**, Cui SJ, Zhang YQ, Xu YY, Hung SC, Fu LP, Pang PP, Gong XY, Jin QY. Predicting Chronic Myocardial Ischemia Using CCTA-Based Radiomics Machine Learning Nomogram. *J Nucl Cardiol*2020 epub ahead of print [PMID: 32557238 DOI: 10.1007/s12350-020-02204-2]

40 **Ridker PM**, Everett BM, Thuren T, MacFadyen JG, Chang WH, Ballantyne C, Fonseca F, Nicolau J, Koenig W, Anker SD, Kastelein JJP, Cornel JH, Pais P, Pella D, Genest J, Cifkova R, Lorenzatti A, Forster T, Kobalava Z, Vida-Simiti L, Flather M, Shimokawa H, Ogawa H, Dellborg M, Rossi PRF, Troquay RPT, Libby P, Glynn RJ; CANTOS Trial Group. Antiinflammatory Therapy with Canakinumab for Atherosclerotic Disease. *N Engl J Med* 2017; **377**: 1119-1131 [PMID: 28845751 DOI: 10.1056/NEJMoa1707914]

41 **Ridker PM**, Libby P, MacFadyen JG, Thuren T, Ballantyne C, Fonseca F, Koenig W, Shimokawa H, Everett BM, Glynn RJ. Modulation of the interleukin-6 signalling pathway and incidence rates of atherosclerotic events and all-cause mortality: analyses from the Canakinumab Anti-Inflammatory Thrombosis Outcomes Study (CANTOS). *Eur Heart J* 2018; **39**: 3499-3507 [PMID: 30165610 DOI: 10.1093/eurheartj/ehy310]

42 **Ross R**. Atherosclerosis--an inflammatory disease. *N Engl J Med* 1999; **340**: 115-126 [PMID: 9887164 DOI: 10.1056/NEJM199901143400207]

43 **Antonopoulos AS**, Sanna F, Sabharwal N, Thomas S, Oikonomou EK, Herdman L, Margaritis M, Shirodaria C, Kampoli AM, Akoumianakis I, Petrou M, Sayeed R, Krasopoulos G, Psarros C, Ciccone P, Brophy CM, Digby J, Kelion A, Uberoi R, Anthony S, Alexopoulos N, Tousoulis D, Achenbach S, Neubauer S, Channon KM, Antoniades C. Detecting human coronary inflammation by imaging perivascular fat. *Sci Transl Med* 2017; **9**: eaal2658 [PMID: 28701474 DOI: 10.1126/scitranslmed.aal2658]

44 **Oikonomou EK**, Marwan M, Desai MY, Mancio J, Alashi A, Hutt Centeno E, Thomas S, Herdman

L, Kotanidis CP, Thomas KE, Griffin BP, Flamm SD, Antonopoulos AS, Shirodaria C, Sabharwal N, Deanfield J, Neubauer S, Hopewell JC, Channon KM, Achenbach S, Antoniades C. Non-invasive detection of coronary inflammation using computed tomography and prediction of residual cardiovascular risk (the CRISP CT study): a post-hoc analysis of prospective outcome data. *Lancet* 2018; **392**: 929-939 [PMID: 30170852 DOI: 10.1016/S0140-6736(18)31114-0]

45 **Oikonomou EK**, Williams MC, Kotanidis CP, Desai MY, Marwan M, Antonopoulos AS, Thomas KE, Thomas S, Akoumianakis I, Fan LM, Kesavan S, Herdman L, Alashi A, Centeno EH, Lyasheva M, Griffin BP, Flamm SD, Shirodaria C, Sabharwal N, Kelion A, Dweck MR, Van Beek EJR, Deanfield J, Hopewell JC, Neubauer S, Channon KM, Achenbach S, Newby DE, Antoniades C. A novel machine learning-derived radiotranscriptomic signature of perivascular fat improves cardiac risk prediction using coronary CT angiography. *Eur Heart J* 2019; **40**: 3529-3543 [PMID: 31504423 DOI: 10.1093/eurheartj/ehz592]

46 **Lin A**, Kolossváry M, Yuvaraj J, Cadet S, McElhinney PA, Jiang C, Nerlekar N, Nicholls SJ, Slomka PJ, Maurovich-Horvat P, Wong DTL, Dey D. Myocardial Infarction Associates With a Distinct Pericoronary Adipose Tissue Radiomic Phenotype: A Prospective Case-Control Study. *JACC Cardiovasc Imaging* 2020; **13**: 2371-2383 [PMID: 32861654 DOI: 10.1016/j.jcmg.2020.06.033]

47 **van Rosendael AR**, Maliakal G, Kolli KK, Beecy A, Al'Aref SJ, Dwivedi A, Singh G, Panday M, Kumar A, Ma X, Achenbach S, Al-Mallah MH, Andreini D, Bax JJ, Berman DS, Budoff MJ, Cademartiri F, Callister TQ, Chang HJ, Chinnaiyan K, Chow BJW, Cury RC, DeLago A, Feuchtner G, Hadamitzky M, Hausleiter J, Kaufmann PA, Kim YJ, Leipsic JA, Maffei E, Marques H, Pontone G, Raff GL, Rubinshtein R, Shaw LJ, Villines TC, Gransar H, Lu Y, Jones EC, Peña JM, Lin FY, Min JK. Maximization of the usage of coronary CTA derived plaque information using a machine learning based algorithm to improve risk stratification; insights from the CONFIRM registry. *J Cardiovasc Comput Tomogr* 2018; **12**: 204-209 [PMID: 29753765 DOI: 10.1016/j.jcct.2018.04.011]

48 **Motwani M**, Dey D, Berman DS, Germano G, Achenbach S, Al-Mallah MH, Andreini D, Budoff MJ, Cademartiri F, Callister TQ, Chang HJ, Chinnaiyan K, Chow BJ, Cury RC, Delago A, Gomez M, Gransar H, Hadamitzky M, Hausleiter J, Hindoyan N, Feuchtner G, Kaufmann PA, Kim YJ, Leipsic J, Lin FY, Maffei E, Marques H, Pontone G, Raff G, Rubinshtein R, Shaw LJ, Stehli J, Villines TC, Dunning A, Min JK, Slomka PJ. Machine learning for prediction of all-cause mortality in patients with suspected coronary artery disease: a 5-year multicentre prospective registry analysis. *Eur Heart J* 2017; **38**: 500-507 [PMID: 27252451 DOI: 10.1093/eurheartj/ehw188]

49 **Johnson KM**, Johnson HE, Zhao Y, Dowe DA, Staib LH. Scoring of Coronary Artery Disease Characteristics on Coronary CT Angiograms by Using Machine Learning. *Radiology* 2019; **292**: 354-362 [PMID: 31237495 DOI: 10.1148/radiol.2019182061]

50 **van Assen M**, Varga-Szemes A, Schoepf UJ, Duguay TM, Hudson HT, Egorova S, Johnson K, St Pierre S, Zaki B, Oudkerk M, Vliegenthart R, Buckler AJ. Automated plaque analysis for the prognostication of major adverse cardiac events. *Eur J Radiol* 2019; **116**: 76-83 [PMID: 31153577 DOI: 10.1016/j.ejrad.2019.04.013]

51 **von Knebel Doeberitz PL**, De Cecco CN, Schoepf UJ, Albrecht MH, van Assen M, De Santis D, Gaskins J, Martin S, Bauer MJ, Ebersberger U, Giovagnoli DA, Varga-Szemes A, Bayer RR 2nd, , Schönberg SO, Tesche C. Impact of Coronary Computerized Tomography Angiography-Derived Plaque Quantification and Machine-Learning Computerized Tomography Fractional Flow Reserve on Adverse Cardiac Outcome. *Am J Cardiol* 2019; **124**: 1340-1348 [PMID: 31481177 DOI: 10.1016/j.amjcard.2019.07.061]

52 **Commandeur F**, Slomka PJ, Goeller M, Chen X, Cadet S, Razipour A, McElhinney P, Gransar H, Cantu S, Miller RJH, Rozanski A, Achenbach S, Tamarappoo BK, Berman DS, Dey D. Machine learning to predict the long-term risk of myocardial infarction and cardiac death based on clinical risk, coronary calcium, and epicardial adipose tissue: a prospective study. *Cardiovasc Res* 2020; **116**: 2216-2225 [PMID: 31853543 DOI: 10.1093/cvr/cvz321]

53 **Kwan AC**, McElhinney PA, Tamarappoo BK, Cadet S, Hurtado C, Miller RJH, Han D, Otaki Y, Eisenberg E, Ebinger JE, Slomka PJ, Cheng VY, Berman DS, Dey D. Prediction of revascularization by coronary CT angiography using a machine learning ischemia risk score. *Eur Radiol* 2021; **31**: 1227-1235 [PMID: 32880697 DOI: 10.1007/s00330-020-07142-8]

Published by **Baishideng Publishing Group Inc**
7041 Koll Center Parkway, Suite 160, Pleasanton, CA 94566, USA
Telephone: +1-925-3991568
E-mail: bpgoffice@wjgnet.com
Help Desk: https://www.f6publishing.com/helpdesk
https://www.wjgnet.com